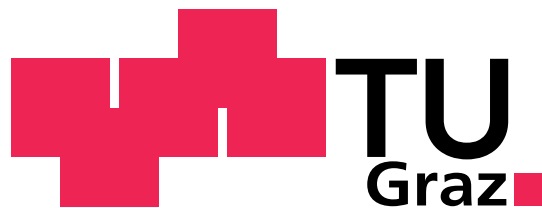


Cheng-Da Ho

Implementation of a Feedback Control for a continuous tubular Crystallizer

Diploma/Master thesis



Institute of Medical Engineering
Graz University of Technology
Kronesgasse 5,A - 8010 Graz
Head: Univ.Prof.Dipl-Ing.Dr.techn.Rudolf Stollberger

Supervisor:
Dipl.-Ing. Dr.techn. B.Sc. Maximilian Besenhard
Research Center Pharmaceutical Engineering GmbH (RCPE)
Inffeldgasse 13, A - 8010 Graz

Dipl.-Ing. BSc. Peter Neugebauer
Graz University of Technology
Institute of Process and Particle Engineering
Inffeldgasse 13, A - 8010 Graz

Evaluator:
Ao.Univ.-Prof. Dipl.-Ing. Dr.techn.Hermann Scharfetter
Graz University of Technology
Institute of Medical Engineering
Kronesgasse 5, A - 8010 Graz

Graz,(October, 2014)

Deutsche Fassung:

EIDESSTATTLICHE ERKLÄRUNG

Ich erkläre an Eides statt, dass ich die vorliegende Arbeit selbstständig verfasst, andere als die angegebenen Quellen/Hilfsmittel nicht benutzt, und die den benutzten Quellen wörtlich und inhaltlich entnommene Stellen als solche kenntlich gemacht habe.

Graz, am
(Unterschrift)

Englische Fassung:

STATUTORY DECLARATION

I declare that I have authored this thesis independently, that I have not used other than the declared sources / resources, and that I have explicitly marked all material which has been quoted either literally or by content from the used sources.

.....
(date) (signature)

Zusammenfassung

Ziel: Ziel dieser Arbeit ist die Realisierung einer Feedback-Regelung an einem vorhandenen kontinuierlichen Schlauchreaktor. Dazu musste eine Umgebung geplant und geschaffen werden, die sowohl hardwaretechnisch als auch softwaretechnisch den Erfordernissen entspricht.

Methoden: Eine Feedback-Regelung konnte mittels eines implementierten Partikelzählers entwickelt und realisiert werden. Dazu wurden sowohl ein Ventil-System, ein Konzept für die Partikelverdünnung als auch die notwendige Software entwickelt. Zusätzlich wurde in Hinblick auf die notwendige Betriebsdauer des Reaktors ein Reinigungskonzept implementiert.

Ergebnisse: Es konnte die Stabilität des Reaktors über einen längeren Zeitraum gezeigt werden. Weiters war es dem Controller möglich, bei zwei unterschiedlich großen Impfkristallen eine Regelung der Produktkristalle auf $140 \pm 2 \mu\text{m}$ durchzuführen. Durch den Feedback Controller konnten Partikelgrößen in einem Bereich von $90 \mu\text{m}$ – $140 \mu\text{m}$ erzielt werden.

Schlussfolgerung: In dieser Arbeit wird ein Konzept präsentiert, welche die Produktion von Partikeln mit gewünschter Größe für einen kontinuierlichen Schlauchreaktor ermöglicht. Basierend auf einer modellfreien Kontrollstrategie war es möglich gewünschte Partikelgrößen konstant und über einen längeren Zeitraum zu produzieren.

Schlüsselwörter: Kristallisation, Kontinuierliche Kristallisation, Kristallgrößen Variation, Online CSD Bestimmung, CSD Regelung, Schlauchreaktor

Abstract

Objective: The aim of the study is the prove of concept of a feedback control loop for a continuous tubular crystallizer. Therefore an experimental set-up for the implementation of a hardware as well a software technical part had to be designed and implemented.

Methods: Due to the implementation of a CSD (crystal size distribution) analyzer, it was possible to develop a feedback controller capable of tuning crystal sizes. For this purpose a measurement environment which contains a valve system, a dilution concept and the development of a control software, was designed and implemented. In addition, a cleaning concept was implemented to provide long term runs.

Results: The results show that for a consistent process set-up the CSD of the product crystals remained constant, that product crystals with the mean size of $140 \pm 2 \mu\text{m}$ were achievable for two different seed suspensions and that the controller was capable of tuning the mean crystal size accurately within a range of $90 \mu\text{m}$ – $140 \mu\text{m}$.

Conclusion: This work demonstrates crystal size tuning in a continuously operated tubular crystallizer via a simple model free control strategy. It was shown that the reproduction of product crystals of a certain mean crystal size over a longer period of time and crystal size tuning were feasible.

Keywords: Crystallization, Continuous Crystallization, Crystal size tuning, Online CSD determination, Feedback control, Tubular reactor

Symbols and Abbreviations

Symbols

$\Delta\hat{G}$	J mol^{-1}	free Gibbs energy
$\Delta\hat{H}$	J mol^{-1}	Entropy
$\Delta\hat{S}$	J mol^{-1}	Enthalpy
μ	J mol^{-1}	Chemical potential
T	$^{\circ}$	Temperature
S	1	Supersaturation ratio
c	mol l^{-1}	Concentration
I	W m^{-2}	Intensity
c_{ext}	cm^2	Cross section
l	cm	Distance of the measuring chamber
m	g	Mass
ρ	g cm^{-3}	Volumetric mass density
P	mbar	Pressure
$\Delta r_{\text{analog-input}}$	mV_{Unit}	Resolution of the Input-Pin of the Arudino Uno board
Δr_{sensor}	bar V^{-1}	Sensitivity of the pressure sensor
L_{mean}	μm	Mean product crystal size
$V_{\text{feed sol.}}$	ml min^{-1}	Pump rate of the feed solution

Abbreviations

PSD	Particle size distribution
CSD	Crystal size distribution
ASA	Acetylsalicylic acid
EtOH	Ethanol
PWM	Pulse-width modulation
ICSP	In-circuit serial programming
USB	Universal serial bus

Contents

1	Introduction	1
1.1	Problem definition / Purpose	3
2	Theory	4
2.1	Crystallization	4
2.1.1	System properties	4
2.1.2	Nucleation	6
2.1.3	Crystal growth	8
2.1.4	Crystallization process	9
2.1.5	Industrial crystallizers	11
2.2	Particle Characterization	13
2.2.1	Particle size distribution	13
2.2.2	Online measurement techniques	16
3	Methods and Materials	19
3.1	Materials	19
3.2	Process Equipment	19
3.3	Hardware	20
3.3.1	Arduino Board	21
3.3.2	Particle counter	22
3.4	Software	24
3.4.1	Particle counter	26
3.4.2	Valve Control	26
3.4.3	Data acquisition, evaluation, control	28
3.4.4	Synchronicity	31
3.5	Seed Generation	34
3.6	Setup and Control	34
3.6.1	Setup	35
3.6.2	Control	38
4	Experimental results	39
4.1	Consistency of the tubular crystallizer	39
4.2	Tuning the mean crystal size to 140 μ m	41
4.3	Stepwise tuning of the mean crystal size	43

5	Discussion	47
5.1	Hardware and setup	47
5.2	Software	50
5.3	Experimental results	52
5.3.1	Consistency of the tubular crystallizer	52
5.3.2	Tuning the mean crystal size to 140 μ m	52
5.3.3	Stepwise tuning of the mean crystal size	53
5.4	Optimization	54
5.5	Conclusion	54

List of Figures

1	Gibbs free energy	6
2	Metastable zone	9
3	Effect of seeding on cooling crystallization	10
4	Forced circulation crystallizer	11
5	Draft tube baffle crystallizer	12
6	Oslo crystallizer	12
7	Forms of distribution	14
8	Light-extinction principle	16
9	Focused beam reflectance measurement	18
10	Process draft	20
11	Valve controlling hardware	21
12	Particle counter	22
13	Feedback control loop	24
14	Software architecture	25
15	Calibration curve	26
16	Schematic of control system	28
17	Response function $L_{\text{mean},q0}(V_{\text{seed}})$	31
18	Synchronicity	32
19	Process Slots	33
20	Seed generation	34
21	Particle size consistency	36
22	Setpoint determination	37
23	CSD for long-run test	39
24	Pressure data for long-run test	40
25	Feedback loop with two different initial seeds	41
26	Pressure data for different seeds experiments	42
27	Micrographs of different seeds experiments	43
28	Stepfunction	44
29	Pressure during step function experiment	45
30	Micrographs of step function experiment	46

List of Tables

1	Types of Weighting	14
2	Technical specification of Arduino Uno	21
3	Technical specification of particle counter	22
4	Calibration data	26
5	Results of the different dilution concepts	36
6	Investigated process settings with used pump rates	37
7	Process settings for the ASA-Crystallization	38
8	Consistency of the measured CSD	40
9	Control history of tuning the mean crystal size to 140 μm	42
10	Control history of stepwise tuning of the mean crystal size	44

1 Introduction

Solid crystals comprise a rigid lattice of molecules, atoms or ions in all three spatial dimension [1]. In fact, they may vary in size and shape. For instance, crystals may appear in the form of a flake or a tetrahedron, but their interfacial angles never change.

Product crystals have an important role in various fields in industry. In the electric industry crystals are used as basic material for the production of microchips or optical components. Crystalline substances may also take an important role in the fine-chemical, pharmaceutical and food industry. In fact, approximately 90 percent of all active pharmaceutical ingredients (API) are organic molecules [2].

Crystallization from solution is a common and important method for phase separation in order to obtain highly purified solids. Besides the purity of crystallized substances, the shape, the size, surface properties and polymorphism are critical indicators for the quality of crystals. In fact, the quality of crystalline substances influences the physical and chemical behavior in regard to their intended application. For instance, in the case of API production the quality includes dissolution and disintegration behavior of the API within the human body [3]. In addition, properties such as flowability, storage characteristics, segregation phenomena, dusting, compatibility, or tabletability depend on the quality [3] [4].

From an economic point the costs and the efficiency of downstream processes like filtration, washing or drying can be optimized by the product quality itself. Therefore, tight process control and optimized process conditions ensure distinguished quality and high profits [5] [6]. Due to the economic importance of the crystallization process, various methods and crystallization types were developed in the past years [7].

In general, crystallizers are classified based on how supersaturation is generated (e.g.

by vaporization, cooling, chemical reaction, ect.) or by the process mode itself (e.g. crystallization in batch, semi-batch or continuous). Besides conventional batch and continuous crystallization systems, innovative basic approaches have been reported like the usage of micro-reactors [8] or impinging jet precipitation, as described by Midler et al. [9] and Brenek et al. [10].

The pharmaceutical industry relies on the usage of batch-systems for the manufacturing of microparticles. These systems have many advantages which are easy implementation and maintenance, suitability for viscous and toxic substances and the ability to obtain larger crystals for systems with slow crystal growth [4]. On the other hand continuous systems have advantages as well which are better control of the optimal process condition, shorter down times, lack of scale-up problems, good reproducibility of products and the possibility of smaller dimensioned reactors which can reduce the required capital and operating costs [7]. Continuous crystallization systems offer a high level of automation and therefore a cost-efficient way for producing APIs.

Besides the advantages of continuous crystallization, potential problems regarding industrial crystallization may appear, namely incrustation problems, slow attainment of a steady-state and potential operational instability. [7].

An example of a continuous crystallization reactor is described in a patent of Schiewe and Zierenberg [11] where inhalable drug particles in a size of $0.3\ \mu\text{m}$ to $20\ \mu\text{m}$ are precipitated through tube-like channels. A stream of alternating segments of a solution and a transport medium induce a very narrow residence time distribution and consequently constant flow of the produced particle size. In addition Mendez del Rio and Rousseau [12] present a tubular device for tubular-batch crystallization where tubing was used for cooling the solution in a direct and rapid way. Crystal particles grew in a stirred vessel after primary nucleation.

Other publications of tubular crystallizers are shown by Eder et al. [13] [14] [15]. The realization of a continuously seeded, continuously operated tubular crystallizer and the impact of different flow rates on product crystals respectively on the crystal size distribution (CSD) for a reactor design as used within this work is presented in [13]. The effect of different seed loadings in respect of the CSD is investigated in [14] where the feasibility of a control strategy is demonstrated.

The objective of most control strategies for crystallizers is to optimize or tune properties related to the CSD or the crystal shape and size distribution (CSSD) what demonstrates their importance [16] [17] [18]. Other control objectives are the minimization of the coefficient of variation, the maximization of the yield [19] [20] or polymorphic purity [21] [22] [23]. Speaking about CSSD control for solution crystallization, the most common optimization variables are temperature trajectories [24] [25] [22] [26] [27] (including temperature cycles [28] [21]), seeding strategies [29] [30] as well as anti-solvent addition rates or combinations of the latter [31] [32]. In a recent approach, the concentration of crystal growth modifiers was used to achieve the desired crystal shape [33].

1.1 Problem definition / Purpose

Continuous crystallization remains a complex challenge in pharmaceutical engineering due to its complexity and dynamic nature. It is highly non-linear along with consisting of a liquid and solid phase. By using tubular reactors it is possible to overcome obstacles like heterogeneous concentration profiles, a slow response to changes of the outer parameters and inaccurate or fluctuating levels of super saturation.

Based on the work of Eder et al. on tubular crystallizers [13] [14] [15] an online measurement system for the determination of the crystal size distribution (CSD) should be designed and implemented to realize a feedback control loop to tune the CSD. Therefore a particle counter for the determination of the CSD has to be established. In addition to the installation of the particle counter, an environment should be planned and implemented which allows the feedback controller to work in a fully automatic way. Besides, the hardware technical part, an appropriate software has to be developed which includes the control of the implemented hardware, the analysis of the measured CSD data, the necessary data processing and the control algorithm of the control system.

2 Theory

2.1 Crystallization

Crystallization is the formation of solid crystals from a solution, a melt or from a vapor phase. In this work the term "Crystallization" is associated with the formation process from a liquid solution to a phase of solid crystalline particles.

For a better understanding of this thesis, an overview of the crystallization process is given in the following sections. The review contains unit operations which are:

- the necessary system properties for crystallization
- nucleation
- crystal growth

In addition, a short overview of commonly used industrial crystallizers is presented in chapter 2.1.5.

2.1.1 System properties

The phase change of a liquid supersaturated solution to a suspension with solid crystal-particles can be explained by thermodynamic principles [34]. In general, the transformation of a phase to another at a constant pressure and temperature induces a change of the chemical potential which is given by the change of the molar Gibbs free energy $\Delta\hat{G}$.

$$\Delta\hat{G} = \mu_2 - \mu_1 \quad (1)$$

μ_2 and μ_1 are the chemical potentials of phase 1 and 2, respectively. When $\Delta\hat{G} < 0$ the transition from state 2 to state 1 occurs spontaneously. The case $\Delta\hat{G} = 0$ defines a state of thermodynamical equilibrium. For $\Delta\hat{G} > 0$ the transition from state 2 to state 1 is only possible under the addition of energy.

To initialize the phase transition and thus nucleation in absence of a solid phase, the free Gibbs energy has to be negative. This correlation is shown in the Gibbs Helmholtz equation which describes the Gibbs enthalpy $\Delta\hat{G}$ as a function of the entropy $\Delta\hat{S}$, the enthalpy $\Delta\hat{H}$ and the temperature T

$$\Delta\hat{G} = \Delta\hat{H} - T \cdot \Delta\hat{S} \quad (2)$$

The molar free Gibbs energy can also be expressed as a function of the saturation ratio of the solution [34]

$$\Delta\hat{G} = -R \cdot T \cdot \ln(S) \quad (3)$$

where R is the universal gas constant, T the absolute temperature and S the supersaturation ratio. The supersaturation ratio S can be expressed by the actual solution concentration c and the equilibrium saturation value c^* .

$$S = \frac{c}{c^*} \quad (4)$$

As can be seen from equation (3) and (4) the degree of supersaturation influences $\Delta\hat{G}$ and thus the process of crystallization, in particular the nucleation rate. In case of supersaturation ($S > 1$) the chance of a spontaneous phase transition is given as $\Delta\hat{G} < 0$. In contrary, for undersaturation ($S < 1$) $\Delta\hat{G}$ takes positive values, thus spontaneous phase transition is not possible.

There are different ways to reach supersaturation in a solution. For systems in which the solubility of the solute increases with temperature, cooling is a convenient way to induce supersaturation. In case for solutions without a high sensitivity to temperature changes, supersaturation can be achieved by evaporation. Another method to induce supersaturation is by adding another component to the reaction environment, thus reducing the solubility of the solution by "salting out" [34].

With the above-mentioned considerations, supersaturation as the driving force in crys-

tallization, in most cases determining the rates of nucleation and growth, was explained. Nevertheless supersaturation alone is not sufficient to control the development of crystals. Before crystals can grow, solid bodies, embryos, nuclei or seeds as centers of crystallization must exist in the solution.

2.1.2 Nucleation

Primary homogenous nucleation

Classical primary homogenous nucleation theory assumes that solute molecules combine to embryos due to stochastic impacts in absence of any solid interface [34]. The overall free energy ΔG of an embryo is defined as the sum of the free volume energy ΔG_v and the free surface energy ΔG_s . In the phase transition the surface energy ΔG_s increases in regard to the surface tension between the embryo and the solution. At the same time ΔG_v decreases.

$$\Delta G = \Delta G_s + \Delta G_v \quad (5)$$

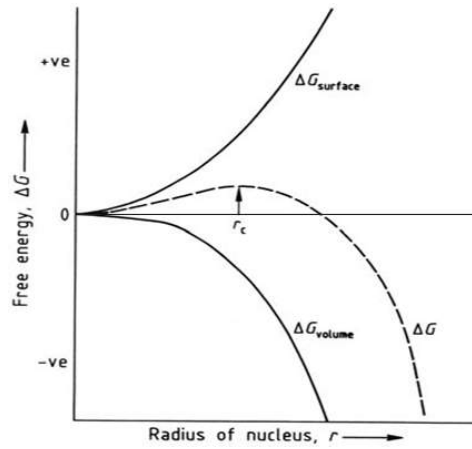


Figure 1: Gibbs free energy in dependency of the radius of the nucleus [35]

Figure 1 shows the behavior of the Gibbs free energy regarding the radius of the nucleus for a supersaturated solution. At a critical particle radius r_c ΔG has a maximum, which determines the activation energy for nucleation. Therefore, to achieve a stable solid phase it is necessary to overcome this "energy barrier", also known as the meta stable

limit. Embryos larger than the meta stable limit remain as macroscopic particles due to the available energy for the creation of a new solid interface ($\Delta G_v > \Delta G_s$). In contrary, particles smaller than the meta stable limit tend to dissolve in the solution.

Primary heterogeneous nucleation

In presence of a solid interface of a foreign seed (e.g. impurities in the system) nucleation is accelerated due to the reduced necessary nucleation energy ΔG caused by the existing surface. This kind of forming nuclei is called primary heterogeneous nucleation. The physical difference between homogenous and heterogeneous nucleation is the limiting maximum nucleation rate, which is for the heterogeneous part limited by the total amount of foreign nuclei [34].

Secondary nucleation

Secondary nucleation occurs when crystals particles of the species under consideration already exist in the crystallizer [35]. In parallel to primary heterogeneous nucleation, the presence of the solid phase (does not have to be of the same crystal structure) can lower the necessary surface energy of the initial nucleus of a specific critical radius. Furthermore the rate of secondary nucleation increases due to the breakage of crystal structures caused by collisions of growing particles with other particles or with internal parts of the crystallizer (e.g. stirrer, wall, pump impeller). In this context properties such as the hardness of the crystal particle or the inner surface of a tubular-crystallizer may have an influence to the increase of crystal fragments. In respect of the collisions of growing particles the density of the solution may also take influence to secondary nucleation due to the higher probability of colliding particles.

Induced nucleation

The generation of uniform crystallization seeds have a profound role for the creation of product crystals. In fact, nucleation events have a stochastic nature and therefore the reproducibility of seeds with the same size may be varied. Especially applications in the industrial field require particles with a narrow particle size distribution.

One method to perform nucleation in a controllable and stable way is the usage of ultrasound. Although the complex mechanism of ultrasound nucleation is not completely understood, it is still used for the creation of uniform and stable particles [36]. In the literature ultrasound nucleation is related to the cavitation phenomenon. The work of

Hem [37] gives an overview about possible aspects which may explain the mechanism behind ultrasound nucleation. Pressure variations, induced by ultrasound, create cavitation bubbles which may collapse when the local static pressure overcomes the vapor pressure of the solution. As a result of the collapse, closely followed by an increase of pressure and temperature, a reduction of the critical radius may happen which accelerates the production of nuclei. Another aspect is the cooling effect which appears when cavitation bubbles are formed. Furthermore, the surface of the cavitation bubble itself acts as a nucleation center which may cause a decrease of the Gibbs free energy and a higher probability of nucleation.

2.1.3 Crystal growth

As soon as a nucleus exceeds a critical size which can be considered as equivalent to a stable nucleus, crystal growth can be observed. In general, crystal growth can be seen as a two-step process where mass transport from the solution to the crystal surface and the integration of growth units into the crystal lattice take place. Several approved growth models exist such as the surface energy model, the adsorption layer model, the kinematic theory, the diffusion-reaction theory and the Burton-Carera-Frank model. For further information of each growth model mentioned see "Crystallization" by J.W.Mullin [1].

In addition, two profound phenomena are discussed in the following due to their influence on the final particle size.

Agglomeration

Small particles in a liquid solution have the tendency to combine into clusters. Thereby particles collide with each other which may cause a permanent attachment and thus an increase of the particle size. This behavior depends on various parameters like the particle size, the level of supersaturation, the particle density or the stir intensity for agitated dispersions. Small particles agglomerate more than bigger particles due to the higher probability for the van der Waals forces to exceed gravitational forces [35].

Ageing

Besides agglomeration the size of particles may be influenced by ripening processes. The so called Ostwald ripening is an phenomenon observed in solutions where smaller

particles have the tendency to dissolve and the solute to be deposited on the larger particles. The explanation for this behavior is the tendency of the system to minimize the total surface free energy which is more favorable for large particles than for small particles [35].

2.1.4 Crystallization process

The process of crystallization contains three main basic steps which are the creation of a supersaturated environment, the generation of nuclei and the corresponding growth of these particles. It has been discussed that supersaturation is the driving force in the process of crystallization without mentioning how nucleation and growth are influenced by the level of supersaturation.

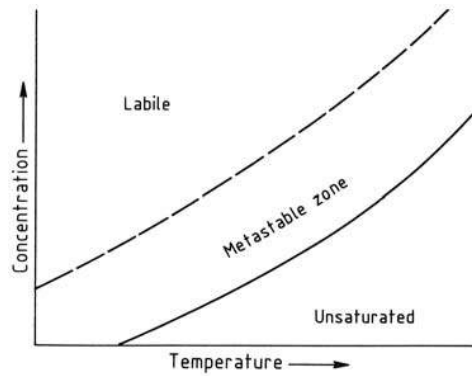


Figure 2: Supersaturation and metastable zone for crystal growth [35]

For supersaturated solutions a regime can be observed where spontaneous nucleation is limited to a minimum and existing crystal particles are growing. This domain is called the metastable zone. Figure 2 shows the solubility changing with to the temperature. For a controlled crystallization process it is essential that the level of supersaturation has to be restricted to the metastable zone. In contrary, a higher level of supersaturation causes a higher amount of spontaneous nucleation and therefore a higher probability of homogenous nucleation. Thus, a controllable crystallization process when creating particles with narrow distribution size is prevented. This behavior occurs in the labile zone above the metastable limit. Below the metastable zone under-saturation prevails where crystals particles are dissolved in the solution.

Based on the aforementioned aspects of an appropriate growing environment, seed crystals can be used to initiate the crystallization process, also known as seeded crystallization. It is a method of controlling crystallization. The main idea of seeded crystallization is the addition of seed crystals into a supersaturated solution whose saturation level lies in the metastable zone at the time of the addition of seeds. Based on the fact that spontaneous nucleation is reduced to a minimum in the metastable zone, the added seed crystals grow by consuming solute. In addition, positive features of seeded crystallization are the reduced amount of fine particles and a narrow particle size distribution. In respect of the final product crystal size, various parameters have influence on the final result during the seeded crystallization process which are:

- Amount of seeds added
- Particle size distribution of the seed crystals
- Growth rate
- Morphology
- Purity
- Mass

The concentration of the solution decreases in parallel to the growth of the crystal particles. Thus, the level of supersaturation is changed with time. Therefore appropriate "cooling rates" have to be established to ensure that the level of supersaturation stays in the metastable zone [35].

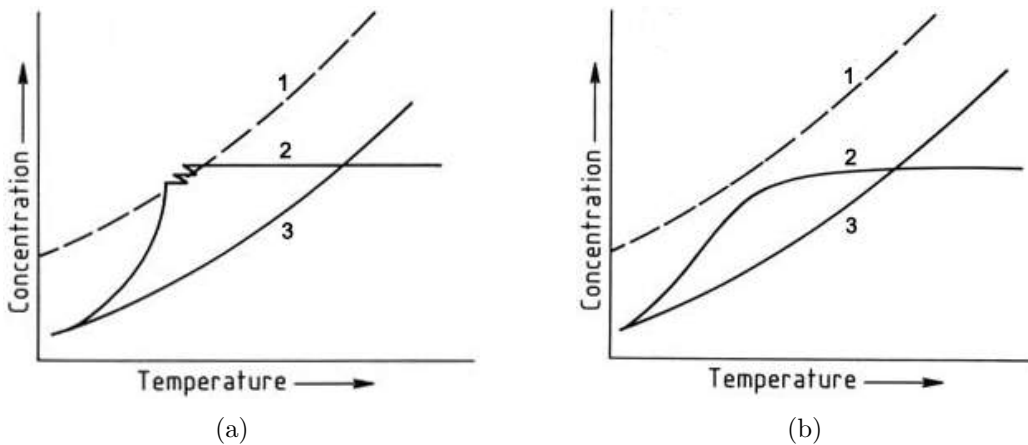


Figure 3: Effect of seeding on cooling crystallization a) Rapid cooling of an unseeded solution [35]; b) Slow cooling of a seeded solution [35]; 1) Supersolubility curve of the solute; 2) Cooling curve of the solution; 3) Solubility curve of the solute

Figure 3a shows the effect of rapid cooling of an unseeded solution. If cooling is performed too fast, nucleation events may occur. Due to the release of latent heat of crystallization an increase of the temperature can be observed, followed by a reiterated decrease of temperature which again induce nucleation. With the number of spontaneous nucleation events it is not possible to control growth and nucleation. A stable and controllable process is shown in Figure 3b.

2.1.5 Industrial crystallizers

This section gives a short overview of commonly used types of continuously operated crystallizers in pharmaceutical industry.

Forced circulation crystallizer

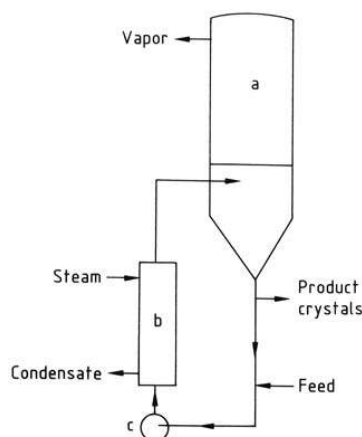


Figure 4: Forced-circulation Swenson crystallizer a) Evaporator; b) Heat exchanger; c) Pump [35]

Figure 4 shows the layout of a forced-circulation crystallizer for a vacuum cooled crystallization. A mix of feed and suspension is pumped through an external heat exchanger into a chamber where crystallization occurs. Due to the addition of heat through the heat exchanger the crystal magma reaches its boiling point and begins to evaporate. Followed by a temperature drop of the liquid solution, supersaturation is reached which starts the crystallization process. The resulting product slurry is withdrawn from the recirculation piping before the feed inlet. Not crystallized crystal magma, which contains small crystal particles together with the solution, is reintroduced into the system. Since crystal particles are infused into the crystal magma mixture spontaneous nucleation is

avoided [35].

Draft tube baffle crystallizer

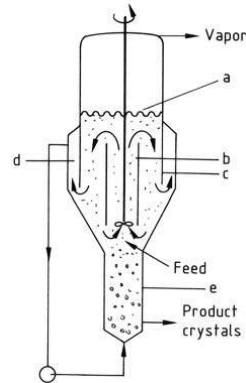


Figure 5: Swenson draft-tube-baffled (DTB) crystallizer a) Boiling surface; b) Draft tube; c) Baffle; d) Settling zone; e) Elutriating leg [35]

The draft tube baffle crystallizer (see Figure 4) is separated into a draft tube and a settling area. An internal baffle prevents agitation effects in the settling area. Hot concentrated feedstock is inserted into the base of the draft tube where a slow-speed agitator is located. Due to the upside flow, induced by the permanently rotating agitator, liquor and crystals from the bottom of the unit are circulated to the liquid surface. At the liquid-vapor interface adiabatic evaporative cooling creates the supersaturated environment necessary for crystal growth. While large crystal particles sediment at the bottom of the settling area, fine particles are extracted and reused to create supersaturation. Final product crystals can be withdrawn from the elutriating leg [35].

Oslo crystallizer

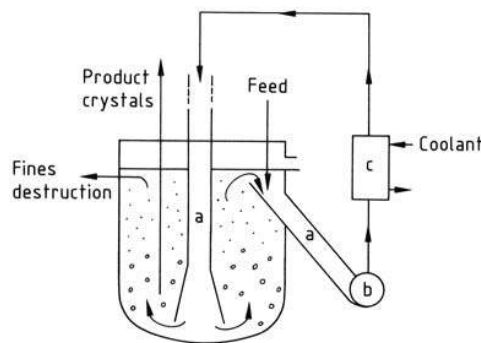


Figure 6: Oslo cooling crystallizer a) Downcomer; b) Pump; c) Heat exchanger [35]

Also known as classified suspension crystallizer, Oslo crystallizers consist of a suspension tank, a downcomer and a heat exchanger which is shown in Figure 6. A mixture of sat-

urated solution and hot concentrated feed solution is pumped through a heat exchanger into the suspension tank where the crystallization process takes place. Supersaturation is induced by direct-contact cooling at the heat exchanger. The solution flows down through the downcomer to the bottom of the tank where the resulting product crystal magma can be collected [35].

2.2 Particle Characterization

Characteristics like the particle size, the shape, surface properties, mechanical properties, charge properties and the microstructure play an important role for the quality in industry. These parameters have a direct influence on the behavior of materials like the reactivity or dissolution rate (e.g. catalysts, tablets), the stability in a suspension (e.g. sediments, paints) or the efficacy of delivery (e.g. asthma inhalers).

The measurement of the particle size is a common critical parameter for the manufacturing of products in a wide range of industry. Due to the fact that particles may have an irregular form in most cases, a characteristic dimension has to be defined. There are different ways to describe the size such as by obtaining the equivalent diameter relating to the geometry (e.g. volume diameter) or by physical properties (e.g. stokes diameter). A good overview about the various definitions of the particle size are shown in [38].

2.2.1 Particle size distribution

The common method for the representation of non-uniform particles with respect to their size and occurrence is the usage of the particle size distribution (PSD).

In practice, the PSD can be presented in form of a frequency distribution curve or a cumulative distribution curve which is shown in Figure 7. Furthermore, the distribution function can be illustrated in form of histograms which are explained in detail [38].

Depending on the measurement principle used for particle analysis (e.g. image analysis, laser diffraction), the particle size distribution can be calculated based on several models

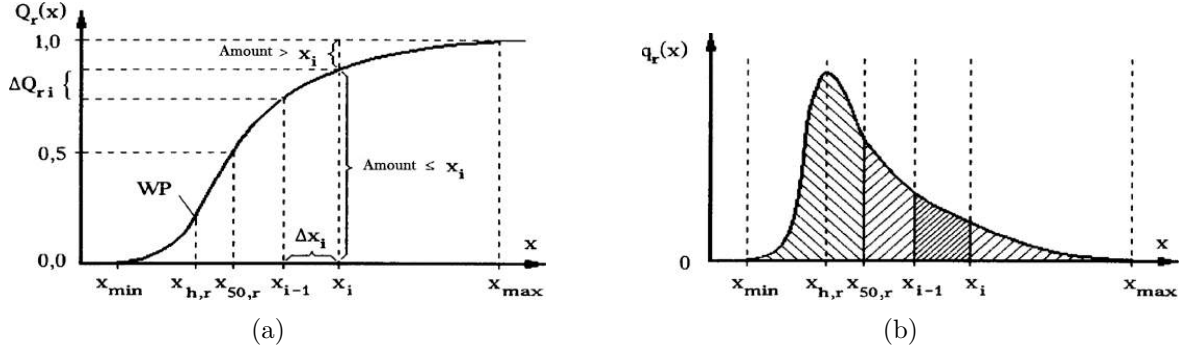


Figure 7: Common representation of the PSD a) Cumulative distribution function [39];
b) Frequency distribution function [39]

[40]. The calculation of the PSD based on a model type will be referred to as weighting henceforth. Table 1 displays the commonly types for weighting [39].

Table 1: Types of Weighting [39]

Index	Type	Distribution
$r = 0$	Number	(x^0) $Q_0(x), q_0(x)$
$r = 1$	Length	(x^1) $Q_1(x), q_1(x)$
$r = 2$	Area	(x^2) $Q_2(x), q_2(x)$
$r = 3$	Volume	(x^3) $Q_3(x), q_3(x)$

By weighting the measured data, different interpretations of the particle size results are possible. For example, a Q_0 weighted PSD only presents the number of particles of different sizes within a batch without regard to the particle geometry. In contrary, a Q_3 weighted PSD includes the spatial distribution of each occurring particle size within the batch. Due to the fact that the volume of bigger particles is higher than that of smaller particles, the probability to detect bigger particles in the batch is higher. Therefore, the Q_3 weighted PSD correlates more likely with the true PSD than the Q_0 weighted PSD. In the pharmaceutical industry a volume based PSD is preferred for most applications [41].

The calculation of the PSD for a cumulative distribution function is shown in Equation 6 [39]. The variables x_{\min} respectively x_{\max} present the limits of a the measured particle size interval and x_i a certain particle size. For a number of N particles, index r defines

the type of weighting (e.g. number, length, area, volume).

$$Q_r(x_i) = \frac{N_r(x_{min} \dots x_i)}{N_r(x_{min} \dots x_{max})} \quad (6)$$

The density function $q_r(x)$ 7 can be derived from equation 6 [39] with the width of a particle size class Δx_i

$$q_{r,i} = \frac{Q_r(x_i) - Q_r(x_{i-1})}{\Delta x_i} = \frac{\Delta Q_{r,i}}{\Delta x_i} \quad (7)$$

It is often useful to describe the PSD with one certain characteristic variable for the representation of the distribution data. Thus the three commonly used values are explained as follows:

Mode

The mode value is the particle size with the maximal occurrence in a density distribution function. In case of two or more maxima the distribution is called bimodal and multimodal, respectively. The mode is marked as $x_{h,r}$ in Figure 7a/b.

Median

The median value is defined as the particle size where 50% of the particle population is below and above that point, respectively. In Figure 7a/b the median is marked as $x_{50,r}$.

Mean

The mean is the center of gravity in a distribution. Referring their frequency, all particle sizes contribute to the calculation of the mean value which is shown in equation 8 [39].

$$\bar{x}_r = \sum_{i=1}^n \bar{x}_i \cdot q_{r,i} \cdot \Delta x_i = \sum_{i=1}^n \bar{x}_i \cdot \Delta Q_{r,i} \quad (8)$$

\bar{x}_i is the average size within a particle size class interval.

2.2.2 Online measurement techniques

This chapter gives a short overview about common particle analyzers which are capable for the online measurement of the particle size distribution in a suspension. In respect of the particle counter used in this work, the measurement principle of the sensor is explained in detail.

Measurements based on light-extinction

Devices based on the light-extinction principle measure the number and size of particles due to the disturbance of the electro-magnetic field in form of light extinction [42]. Figure 8 shows the principal setup of such a device. It consists of three main parts, which are a

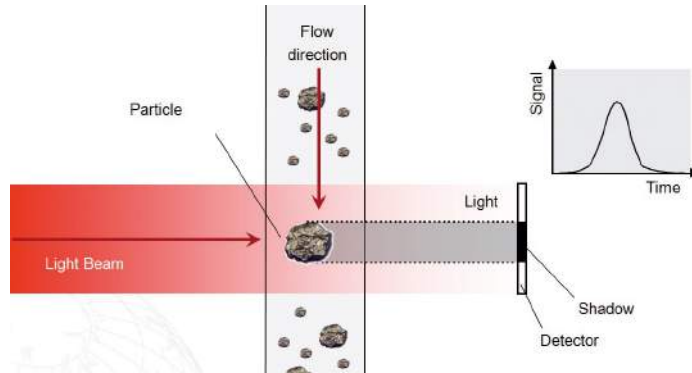


Figure 8: Light-extinction principle: the attenuated light beam is measured through the measuring cell on a photo-detector [43]

light source, a measuring cell and a photo-detector. A collimated light beam is directed to the photo-detector through the measuring cell ($V_{\text{cell}} = 1 \text{ mm}^3$), where the suspension with the particles to be measured are passing. Whenever a particle is crossing this cell, the intensity of the detected light decreases in respect of the level of reflexion, absorption and scattering. As a result a decreased signal can be measured on the detector.

The attenuation of the light beam can be estimated with the Beer-Lambert law in equation 9 where I presents the light intensity measured on the detector, I_0 the intensity before entering the measuring chamber, C_{ext} the cross section, c_0 the number concentration of particles in the measurement chamber which is for the particle sensor used equal 1 and l the length of the light beam through the chamber [39].

$$I = I_0 \cdot e^{-C_{\text{ext}} \cdot c_0 \cdot l} \quad (9)$$

Before the size of particles within a suspension is measured, a calibration of the particle sensor has to be established. Therefore spherical latex particles with a mono-disperse size distribution (e.g. 50 μm , 100 μm) are used. For each mono-disperse particle size used, the attenuated signal of the light beam is measured and recorded in form of data-points of a calibration function. This function describes the attenuation of the light signal in dependency of the particle size measured.

During the measurement of a suspension, the intensity measured on the detector, caused by the particles within the measurement chamber, is compared to the calibration function. The particle size is obtained by matching the value of the signal measured with the value in the calibration function.

For the proper usage of the particle counter it is essential that the concentration of the suspension is kept as low as possible. With the decrease of the suspension concentration, the measurement of bigger particles sizes, caused by overlapping particles, can be avoided [39]. In addition, a known flow velocity through the sensor provides a proper differentiation of following particles.

Measurements based on image analysis

The PSD of a suspension is calculated by the analysis of microscopy pictures. Therefore pictures of the suspension are taken by a camera system and converted subsequently into a greyscale image. In a further imaging process, the size of all occurring particles within the picture are measured. Depending on the used algorithm for the determination of the particle size (i.e. the particle size is defined as the diameter of a circle or the length of a rod) the PSD is finally calculated. For further information see [39].

Measurements based on focused beam reflectance measurement (FBRM)

Instruments based on the principle of the FBRM are capable for the online measurement of particles within a suspension. Figure 9 shows the schematic of a FBRM sensor.

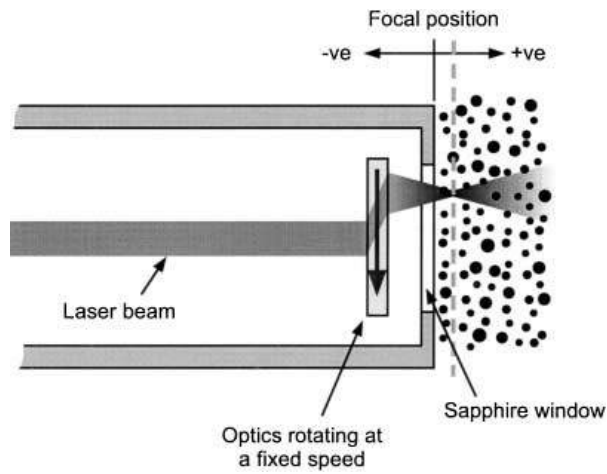


Figure 9: Schematic of FBRM [44]

A monochromatic light beam is focused through a high rotating lens to a specific focus point near the probe. When a particle crosses the light beam, light is reflected back to the sensor. The size of the particle is determined by the duration of the reflected light pulse. For further information see [44].

3 Methods and Materials

3.1 Materials

G.L Pharma GmbH provided the acetylsalicylic acid (Rhodine 3020, pharmaceutical grade, $M = 180.16 \text{ g/mol}$). Ethanol (96% denaturized with 1% methyl ethyl ketone, $M = 46.07 \text{ g/mol}$) was purchased from Roth (Lactan). Polysiloxane tubings with an inner diameter (d_{in}) of 2.0 mm and an outer diameter (d_{out}) of 4.0 mm were used for the tubular reactor. Straight and Y-fittings (PTFE, $d_{\text{in}} = 2.0 \text{ mm}$) were used to assemble the tubular reactor. Filtration was performed using filter cycles with pore sizes of $>4 \mu\text{m}$ (Carl Roth-MN 616).

3.2 Process Equipment

Three peristaltic pumps, P I (Ismatec Reglo MS 2/6V 1.13C; tubing: PHARMED® $d_{\text{in}} = 2.8 \text{ mm}$, $d_{\text{out}} = 5.0 \text{ mm}$) P II (Reglo Digital MS-2/6V 1.13C; tubing: PHARMED® $d_{\text{in}} = 2.8 \text{ mm}$, $d_{\text{out}} = 5.0 \text{ mm}$) and P III (Heidolf Pumpdrive 5106; tubing: silicon $d_{\text{in}} = 1.6 \text{ mm}$, $d_{\text{out}} = 4.8 \text{ mm}$) as well as a gear pump P IV (Ismatec MCP-Z Process IP65) were used to operate the tubular reactor and the CSD analyzer. Magnetic (M&M international; 8250 24/DC) as well as tube pinch valves (Fluid Concept; Sirai S105) were used to switch between process and measuring or cleaning mode. The temperature was controlled via five thermostatic bathes: BI-BIV (LAUDA Type E 111 Ecoline Staredition LAUDA A 24). The sonication during seed generation was performed in an ultrasonic bath (Elma Transonic 460; 35 kHz). The pressure within the tubing was recorded with the aid of a piezoelectric probe (Hygrosens, DRTR-AL-10V-R1B6). The CSD was measured using the Particle counter TCC® (Markus Klotz GmbH) equipped with a 1 mm^3 measuring

chamber. A single-board microcontroller (Arduino; Arduino Uno) handled the control of the valves and the communication with the pressure sensor. A USB to RS232 Adapter (LogiLink®) was used for updating the pump rate during the feedback loop process. Process control and monitoring was governed by MATLAB (Mathworks Inc., Natwick, USA).

3.3 Hardware

This section describes the hardware technical adaption of the existing tubular reactor necessary for the implementation of a continuous feedback control loop. A schematic of the tubular crystallizer setup is shown in Figure 10.

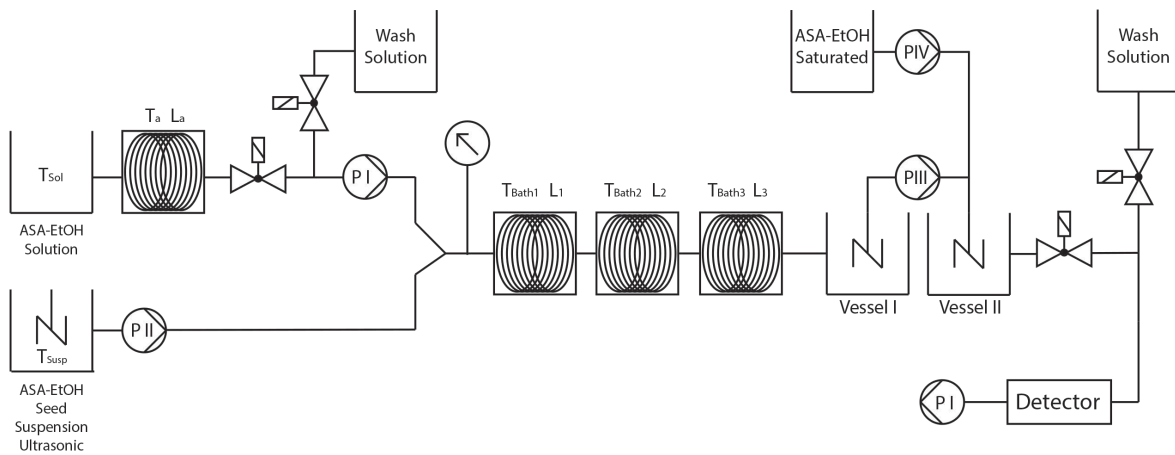


Figure 10: Schematic process draft of the tubular crystallizer containing a cleaning-, dilution- and measurement-system

An environment for online measurements had to be designed and developed which included the implementation of a particle counter, a valve system and a dilution procedure. A tube pitch valve and a magnetic valve were used to introduce into the particle counter the product crystals and the wash solution (EtOH), respectively. A peristaltic pump (PIII) and two vessels were used for the dilution procedure. Due to incrustations within the tubing, the crystallizer was rinsed with a solvent (e.g. EtOH) in regular intervals. Thus, two magnetic valves were implemented. Via an USB to RS232 adapter, the pump rate of the seed suspension was electronically controlled. A pressure sensor was implemented for process monitoring.

3.3.1 Arduino Board

The Arduino Uno is a microcontroller board based on the ATmega328. It has 14 digital input/output pins (of which 6 can be used as PWM outputs), 6 analog inputs (10bit resolution), a 16 MHz ceramic resonator, a USB connection, a power jack, an ICSP header, and a reset button [45]. Table 2 shows a small summary of the technical specifications of the Arduino Uno board.

Table 2: Technical specification of the Arduino Uno [45]

Parameter	Description
Microcontroller	ATmega328
Operating Voltage	5 V
Input Voltage (recommended)	7 V–12 V
Input Voltage (limits)	6 V–20 V
Voltage limits on I/O Pin	–0.5 V–5.5 V
DC Current per I/O Pin	40 mA
DC Current for 3.3 Pin	50 mA



(a)



(b)

Figure 11: a) Arduino board; b) Relay board

The Arduino Uno board was used for the control of the valve systems and the pressure measurement of the reactor via MATLAB (Mathworks Inc., Natwick, USA). The power supply of each valve was controlled by a relay board [46] (see Figure 11) which again was connected to one of the Arduino Uno digital output pins. The rated voltage of the relay was at 1.5 V. The pressure sensor was connected to one of the analog input pins.

Due to the maximal allowed input voltage, a simple voltage divider (two $1\text{ k}\Omega$ resistors in series) was implemented.

3.3.2 Particle counter

The particle counter TCC®(Markus Klotz GmbH) works on a light-extinction principle which is described in chapter 2.2.2. The device consists of a detector and a data acquisition unit which is shown in Figure 12.



Figure 12: a) Particle counter [47]; b) Data acquisition unit [48]

Table 3 shows the technical data of the particle counter.

Table 3: Technical specification the of particle counter [47]

Parameter	Description
Model	LDS 70/70
Flow rate	20 ml min^{-1}
Measuring range	$5\text{ }\mu\text{m} - 500\text{ }\mu\text{m}$
Dimension measuring chamber	$1000 \times 1000\text{ }\mu\text{m}$
Maximal particle concentration	4000 ml^{-1}

Due to the high density of product crystals in the process stream, a dilution process had to be established before CSD measurements were taken. The dilution process was realized by fractional sampling of product crystals from the crystallization process. Subsequently, product crystals were pumped (PIII) with a rate of 6 mL min^{-1} from vessel I to vessel II. A saturated ASA-EtOH solution was pumped via a gear pump (PIV) into vessel II in order to dilute the product crystals. The pump rate of the gear pump

(PIV) was calculated based on the mass fraction of ASA per gram slurry produced. The following calculations present the required dilution for particles with a mono-disperse size distribution.

$$m_{slurry} = m_{ASA} + m_{EtOH} \quad (10)$$

Equation 10 describes the composition of a slurry which consists of ASA and EtOH. The mass fraction of ASA for 1 g slurry of the seed solution with a concentration of $c_{seed\ susp.} = \frac{0.3\text{gASA}}{\text{gEtOH}}$ can be calculated, based on the assumption in formula 10

$$m_{slurry} = m_{ASA_{seed}} + \frac{m_{ASA_{seed}}}{0.3} \rightarrow \frac{m_{ASA_{seed}}}{m_{slurry}} = \frac{1}{(1 + \frac{1}{0.3})} \quad (11)$$

The same calculation can be performed for the feed solution with a concentration of $c_{feed\ sol.} = \frac{0.45\text{gASA}}{\text{gEtOH}}$. Depending on the pump rate of the seed suspension and feed solution, the total amount of ASA for 1 g slurry from the reactor is given

$$\frac{m_{ASA_{reactor}}}{m_{slurry}} = \alpha \cdot \frac{m_{ASA_{feed}}}{m_{slurry}} + \beta \cdot \frac{m_{ASA_{seed}}}{m_{slurry}} \quad (12)$$

where α and β present the pump rate of the feed solution and the seed suspension, respectively in dependency of the total flow rate through the crystallizer. At a temperature of 22°C for 1 g m_{slurry} the mass of dissolved ASA is 0.18 g which is the saturation concentration of ASA in EtOH based on the solubility curve obtained in [49]. Thus, the total amount of solid ASA particles for 1 g m_{slurry} is:

$$\frac{m_{ASA_{solid}}}{m_{slurry}} = \frac{m_{ASA_{reactor}}}{m_{slurry}} - 0.18 \quad (13)$$

With a measuring chamber of a volume $V_{chamber}$ of 1 mm³, the density of ASA $\rho_{ASA} = 1.35\text{ g cm}^{-3}$ and a particle size d_p , the maximally allowed density for CSD measurements is described in the following equation 14

$$\rho_{max} = \frac{d_p^3 \cdot \rho_{ASA}}{V_{chamber}} \cdot 4 \quad (14)$$

The factor 4 in equation 14 is taken from the manufacturer's datasheet for the maximal allowed particle concentration of the particle counter. Based on the aforementioned considerations and assuming a density of the slurry $\rho_{slurry} = 1\text{ g cm}^{-3}$, the level of dilution

can be calculated from equation 13 and 14

$$Dilution = \frac{\rho_{max}}{\frac{m_{ASA_{solid}}}{m_{slurry}} \cdot \rho_{ASA}} \quad (15)$$

As an example, for crystal products with a mono-disperse size distribution of 150 μm , a seed pump rate of 6 ml and a feed pump rate of 20 ml, an eightfold dilution has to be established at least to prevent the measurement of overlapping particles and thus a erroneous crystal size.

3.4 Software

This chapter describes the realization of the feedback control loop which is illustrated in Figure 13.

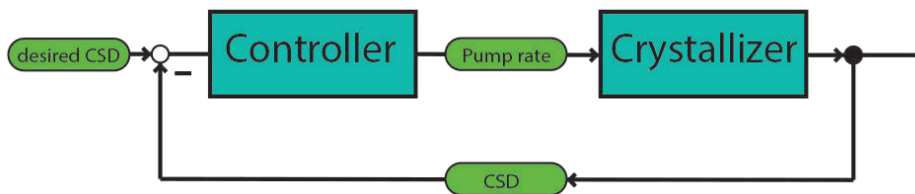


Figure 13: Principle of the feedback control loop

Based on the results of CSD measurements, the controller tries to calculate an appropriate pump rate for a desired mean crystal size. This procedure is repeated until a threshold is undercut for the target mean crystal size.

The feedback control was realized by the implementation of three main tasks which are:

- the CSD measurement of the product crystals
- the control of the valve systems
- the data acquisition and evaluation, followed by a control response.

Each task was executed in parallel with an individual iteration rate which is described later in this chapter (see chapter 3.4.4). Figure 14 shows the scheme of the software

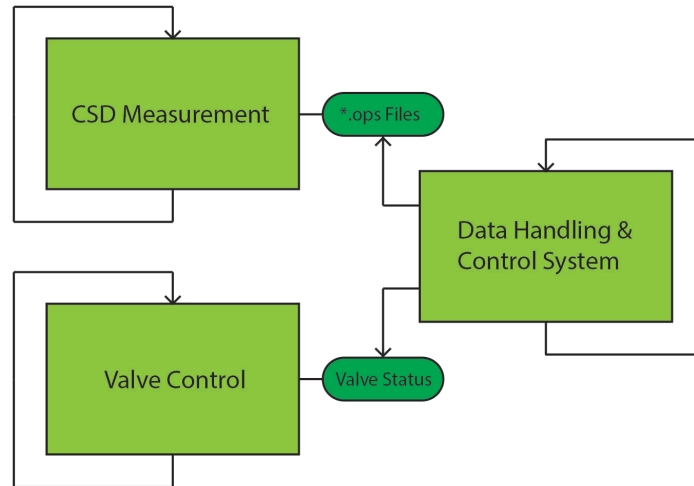


Figure 14: Scheme of the three parallel working tasks for the handling of the feedback control

design.

In regular intervals CSD measurements were conducted and saved on a local server for further processing. At the same time the control of the valves was managed by the "valve control" unit. Besides the control of the valves, the current status of the crystallizer's valves was reported in form of a status variable. In addition, the pressure within the crystallizer was continuously recorded via the pressure probe. The last task represents the central part of the feedback control loop. By obtaining the CSD measurements and the status variable, data acquisition, evaluation and control system were executed in the last task.

In the following sections the software technical realization for each task is described in detail. The MATLAB (Mathworks Inc., Natwick, USA) source code can be taken from the appendix.

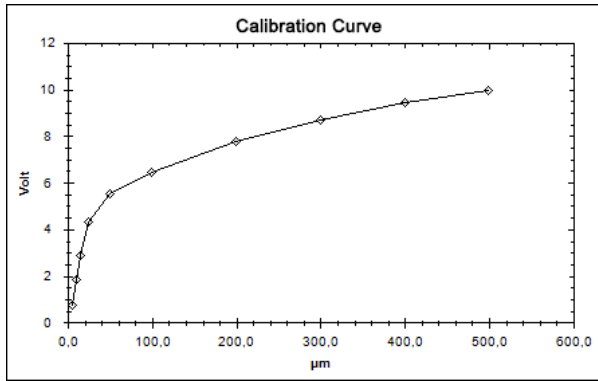


Figure 15: Calibration curve containing the particle size to the referring voltage based on the values in Table 4 taken from the measurement of latex particles

Table 4: Calibration data

Particle diameter d_p [μm]	Cal. Pulse [mV]
5	718
10	1839
15	2879
25	4301
50	5499
100	6431
200	7763
300	8679
400	9404
500	9971

3.4.1 Particle counter

The CSD measurement was performed by the manufacturer's software Protrend (Markus Klotz GmbH). The particle counter was calibrated with the values shown in Table 4. The duration of each measurement was set up to 20 s in an interval of 50 s. As mentioned before, the CSD measurements were transferred to a local server for the further process of the feedback control system.

3.4.2 Valve Control

The Arduino Uno board includes an integrated development environment (IDE) which is designed to simplify programming. Arduino programs or codes, also known as "sketches", are written in C/C++.

The program for the valve timing was written in MATLAB (Mathworks Inc., Natwick, USA). For this reason, a sketch for the communication between MATLAB and the Arduino Uno board was uploaded to the flash memory of the board via the IDE Interface. The sketch can be downloaded from the MATLAB manufacturer's site [50].

The first part of the program contains the initial setup of the Arduino Uno board in

MATLAB. Via the `pinMode()` function specific pins can be configured to behave as an input or output channel.

```

1 %Initiate Arduino Board
2 ard = arduino('COM4');
3 %Setup I/O pins
4 pinMode(ard,9,'OUTPUT') %valve detector sample probe
5 pinMode(ard,10,'OUTPUT') %valve detector wash solution
6 pinMode(ard,5,'OUTPUT') %valve crysallizer feed solution
7 pinMode(ard,6,'OUTPUT') %valve crystallizer wash solution

```

The control of each individual valve was provided by the the `digitalWrite()` function. A logical HIGH (1) and logical LOW (0) level, respectively, opened and the closed the valves.

```

1 %Start Sample to detector
2 digitalWrite(ard,10,0) %close Valve EtOH
3 digitalWrite(ard,9,1) %open Valve Products

```

After each switch of the valves, the pressure signal obtained from the pressure probe was recorded using the `analogRead` function().

```

1 %read pressure
2 pres = analogRead(ard,0);
3 pres_bar(i) = 1.568*pres;

```

The function `analogRead()` returns integer values between 0 and 1023 which represent voltage values between 0 and 5 V. Thus, the calculation of the pressure value is given in equation 16

$$p_{crystallizer} = u \cdot \Delta r_{analog-input} \cdot \Delta r_{sensor} \quad (16)$$

where u describes the obtained integer value, $\Delta r_{analog-input}$ the resolution of the analog input ($=4.9 \text{ mV}_{Unit}$ [51]) and Δr_{sensor} the sensitivity of the pressure sensor ($=0.32 \text{ bar V}^{-1}$ [52]).

The variable `status_val_pro` represented the valve status of the crystallizer which was

updated after switching the valves. The valves for the sampling of product crystals and the cleaning of the particle counter were opened for 30 s and 40 s, respectively. In an interval of 7 min the crystallizer was rinsed with EtOH. The time intervals between these cleaning steps will be referred to as slots henceforth.

3.4.3 Data acquisition, evaluation, control

The evaluation of the measured CSD data with the corresponding feedback control response was established in MATLAB. Figure 16 shows the schematic procedure of necessary working steps.

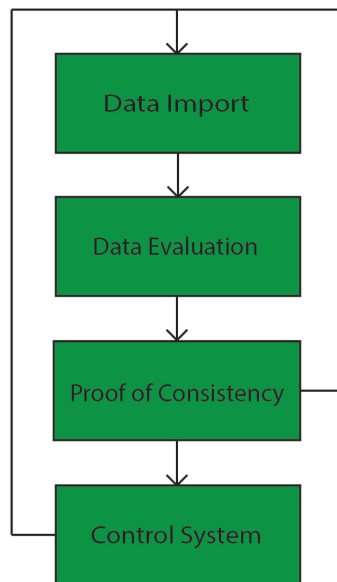


Figure 16: Procedure of the control system script containing the import and evaluation of the CSD data and the subsequent verification of the consistency of the last three measurements

Prior to each iteration, the control program checked the valve status *status_val_pro* of the crystallizer to clarify the presence of product particles in the crystallizer. In case of a cleaning procedure in the tubular reactor, the controller was paused for a certain time which is described later in chapter 3.4.4.

Data import / Data evaluation

In the first step, the CSD measurements were taken from the local server. The Q0 crystal size distribution and the corresponding arithmetic mean, which are described in chapter 2.2.1 (equation 7/8), were calculated for the evaluation of the CSD measurements.

Subsequently the consistence of the CSD measurements had to be investigated before the control system could work. Thus, the last three CSD measurements within a slot were used and analyzed. In order to screen for bad CSD measurements (e.g., because of insufficient dilutions in the measuring chamber or the tubular crystallizer had not yet reached its steady state) the CSDs recorded within a single slot were evaluated by three tests:

1. X^2 Test
2. Comparison of the mean crystal size
3. Comparison of the number of measured particles

The X^2 Test was conducted with the formula 17

$$X^2 = \sum_{j=1}^m \frac{(N_j - n_{0j})^2}{n_{0j}} \quad (17)$$

where N describes the observed frequency, n_0 the expected frequency, m the number of measurements and X^2 the test variable. For the test, the CSD was represented by only 20 equally (not 40 as usual) sized bins between $i_{\min}=35\mu\text{m}$ and $i_{\max}=425\mu\text{m}$. The expected number of particles was obtained by fitting a log-normal distribution through the measured CSD. Thus, a model of the log-normal distribution was created with the MATLAB function `lognpdf()`. Due to the fact, that CSD measurements don't perfectly fit to a log-normal distribution, the chi-value for passing the test was evaluated solely by the results of initial studies at the beginning of this work. A chi-value of 1 was defined as threshold value.

The second test analyzed the calculated mean crystal size L_{mean} of the last three CSD measurements. Therefore L_{mean} was determined by averaging the mean crystal sizes (see equation 8) of the three CSD measurements recorded within one slot. Measurements

within a range of 3 μm were taken as reliable. (see Equation 18)

$$\Delta L_{limit} \geq |L_j - \frac{1}{m} \sum_{j=1}^m L_j| \quad (18)$$

Finally, the number of measured particles was evaluated for the last test. Regarding the concentration of product slurries within the particle counter, the number of product crystal particles was restricted to 30000. By exceeding the limit, the CSD measurement would be discarded due to the higher probability of overlapping particles and thus the measurement of erroneous particle sizes.

In case that three consecutive taken CSD measurements agree within a certain confidence interval, the controller calculated the required change of the seed pump rate in respect to the deviation between the current mean product crystal size and the target size. Otherwise the last CSD was discarded. Once the new pump rate had been calculated, the controller modified the current seed pump rate via the MATLAB function `fprintf()` in the succeeding slot. Hence, the feedback control of the tubular crystallizer was executed from slot to slot.

Controller

Several process settings (e.g. feed rate, temperatures, seed loadings, etc) can be used to influence the product crystals mean diameter L_{mean} as discussed in [13] [14] [49]. Both the flow rates of the feed solution and the seed suspension seem to be the most suitable control variables, not least because they can be changed conveniently.

Initial studies were performed to evaluate the impact of alterations in the pump rate of the seed suspension on the mean crystal size. The CSD and $L_{mean,q0}$ were recorded for five different seed suspension pump rates using the same seed-batch (see Figure 17).

Thereby, a generic response function $\tilde{L}_{mean,q0}(V_{seed})$ was defined to adjust \dot{V}_{seed} according to the deviation between target the crystal size $L_{mean,q0 \ target}$ and the measured crystal size $L_{mean,q0 \ measured}$. First, the crystal size L_{i+1} was calculated by adding the deviation in crystal size to the response function's value at the current seed suspension pump rate ($V_{seed \ i}$), see Equations 19-20. The new seed suspension pump rate ($V_{seed \ i+1}$) follows from the value assigned to the response function at L_{i+1} see equation 21.

$$\epsilon = L_{mean,q0 \ target} - L_{mean,q0 \ measured} \quad (19)$$

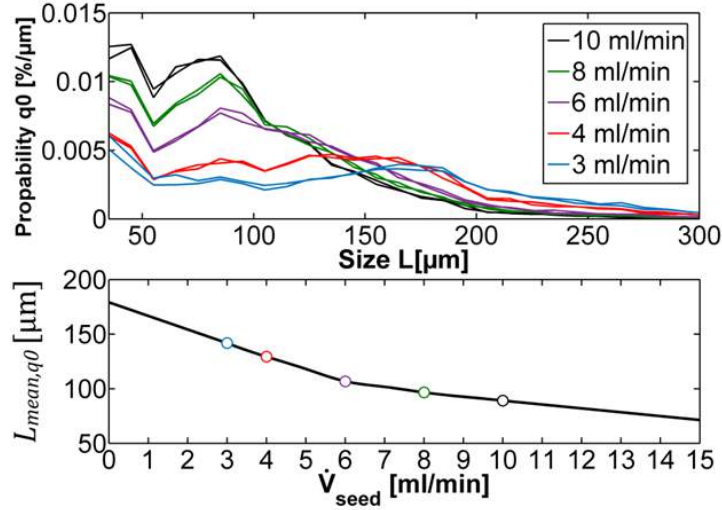


Figure 17: Determination of the response function $L_{\text{mean,num}}(V_{\text{seed}})$ *Top*: CSDs recorded for five seed suspension pump rates (two per setting); *Bottom*: Response function obtained by linear interpolation and extrapolation between and beyond the (averaged) measured mean crystal sizes.

$$L_{i+1} = \tilde{L}_{\text{mean},q_0}(V_{\text{seed}i}) + \epsilon \quad (20)$$

$$\tilde{L}_{\text{mean},q_0}(V_{\text{seed}i+1}) = L_{i+1} \rightarrow V_{\text{seed}i+1} \quad (21)$$

In case of a deviation of $\epsilon \leq 3$ the controller was terminated without any modification of the current seed pump rate which means that the production of the target particle size was accomplished.

The response function was obtained solely from experiments using the same seed-batch, which is a simplification since L_{mean,q_0} depends strongly on the seed crystal attributes. The mentioned experiments are described later in chapter 3.6.1.

Nevertheless this simple feedback control strategy remains applicable as long as the mean crystal size response on the seed suspension pump rate exhibit a strict monotonic decrease, i.e. higher pump rates yield smaller mean crystal sizes.

3.4.4 Synchronicity

Due to the parallel working tasks of the measurement process (see Figure 14), it was necessary to align each individual task to provide a fully-automated measurement and

control process. Thus, two main aspects of synchronization had to be considered which are

- the interplay between the valve control and the CSD measurement
- synchronicity of the wash procedure of the crystallizer and the feedback controller

Valve control - particle counter

The particle counter was rinsed with EtOH to dissolve adhered ASA particles in the measuring chamber of the particle counter between subsequent CSD measurements. The timing of conducting the measurement and switching the valves is shown in Figure 18.

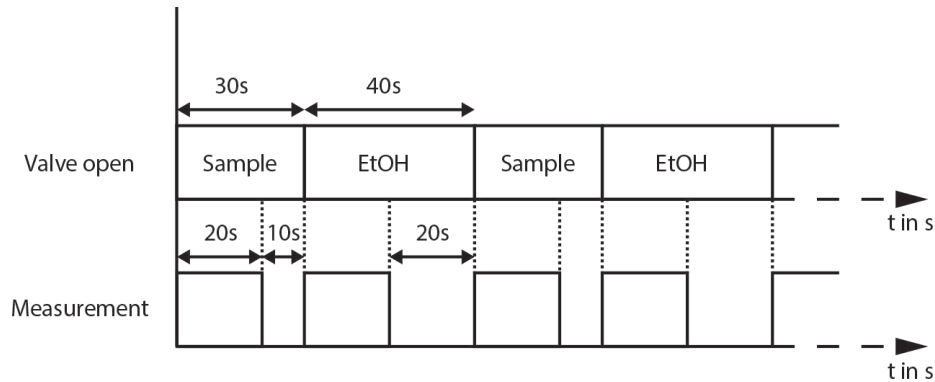


Figure 18: Measuring procedure of the particle counter during the infuse of product samples respectively EtOH into the sensor. Measurements are taken for 20s, starting at the moment when product samples respectively EtOH are infused into the sensor

The CSD measurement of the product crystals started when the pitch tube valve for the sampling was opened for 30s. The duration of the CSD measurement was set to 20s. Subsequently the detector was rinsed with EtOH for 40s. Measurements of the wash solution were taken for control purposes. To ensure that only the suspension of product crystals was passing the particle counter, a puffer-zone of 10s prevented the measurement of mixture of sample and EtOH.

Valve control - controller task

As mentioned before (see Section 3.4.3) the feedback control worked from slot to slot due to the required washing procedure of the crystallizer.

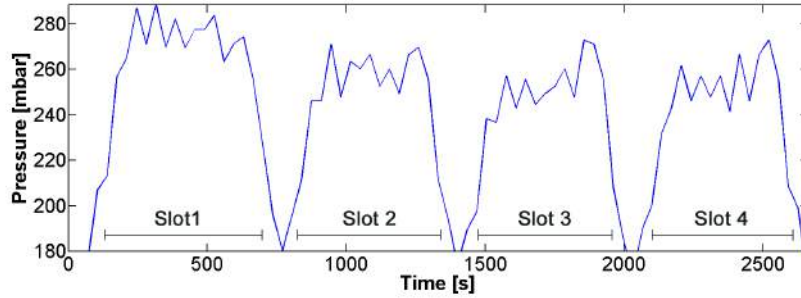


Figure 19: Pressure within the crystallizer during three washing procedures between 4 slots

Figure 19 shows the pressure recorded within the crystallizer during a crystallization process. Due to the short duration of one slot and the delay in the crystallizer, the effects of the new pump rate could only be seen in the following slot. Therefore the slot-status, respectively, the valve status of the crystallizer was continuously recorded in the variable *status_val_pro*. Based on the timing of the wash process, the corresponding duration of the wash cycle (t_{wash}) and the current pump rates ($v_{feed} + v_{seed}$), an expected time was calculated and used to restart the feedback controller.

$$t_{restart} \approx t_{wash} + \frac{V_{tube}}{v_{feed} + v_{seed}} \quad (22)$$

3.5 Seed Generation

In order to have sufficiently small seed crystals with a low fraction of fines ($<5\mu\text{m}$) an ultrasound-assisted seed generation method was used. A schematic draft of this method and a micrograph of generated crystals are shown in Figure 20.

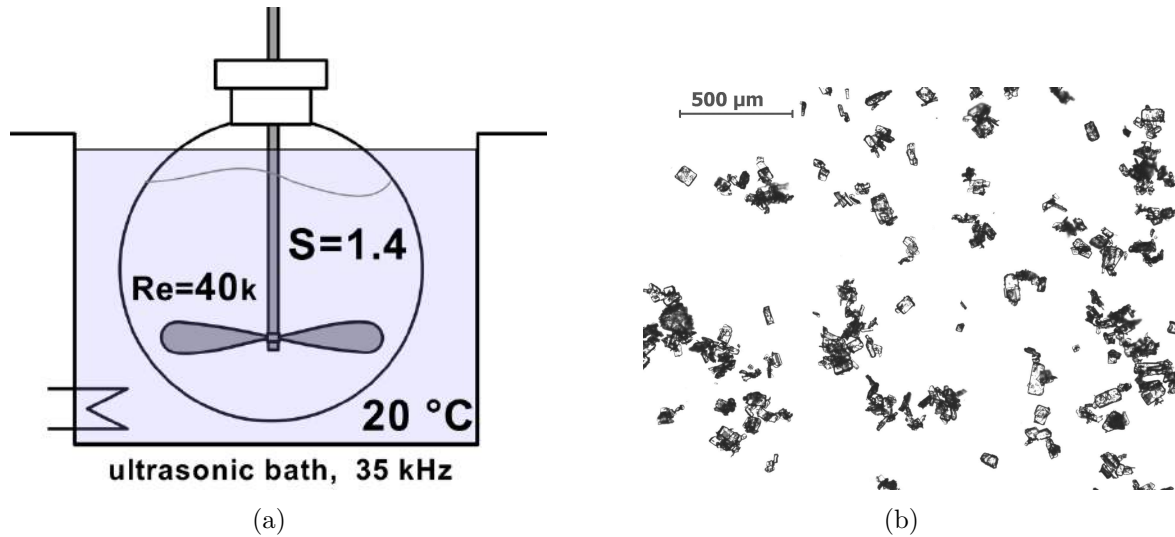


Figure 20: Schematic of the seed generation procedure via sonocrystallization. (b) Micrograph of seed crystals

ASA was dispersed in EtOH with a ratio of $c_{\text{seed susp.}} = 0.3\text{ g}_{\text{ASA}}\text{ g}_{\text{EtOH}}^{-1}$ and dissolved at $\approx 40\text{ }^\circ\text{C}$ in a 500 mL round bottom flask. Subsequently, the solution was cooled to $20\text{ }^\circ\text{C}$ before starting ultrasound irradiation at 35 kHz. At this temperature the solution had a level of supersaturation of $S=c/c^* = 1.4$. The ultrasound irradiation was stopped 45 s–60 s after the first evidence of precipitation (e.g. the solution became slightly milky). Longer irradiation times yielded smaller seed crystals and vice versa. Each seed generation run will be referred to as seed-batch within this work.

3.6 Setup and Control

The first part of this chapter describes the determination of an appropriate setup for the feedback control loop. Three main experiments were subsequently conducted to

demonstrate the automated production of crystal particles based on the feedback control strategy. The control of the crystallizer is described in the second part of this chapter.

3.6.1 Setup

Initial studies were conducted to determine an appropriate dilution method and process setting so that, respectively, the feedback control could be implemented. The experiments with the corresponding results are described in the following.

Analysis of dilution methods

Two variants of dilution were implemented and compared with respect to a stable measurement process. CSD measurements were evaluated to investigate the consistency of the measurement process for both dilution methods. The similar process settings, listed in Table 7, were used for both experiments, except that $c_{\text{feed sol.}} = 0.40 \text{ g}_{\text{ASA}} \text{ g}_{\text{EtOH}}^{-1}$ was changed. The tubular crystallizer was operated for about 45 min.

The fractional sampling of the product slurry was realized by the installation of a Y-fitting at the end of the process (Experiment 1). In contrast, the second dilution method (Experiment 2) consisted of two vessels and a peristaltic pump.

By placing the Y-fitting at the end of the process, the amount of product crystals was divided in half. Subsequently, one half of the product crystals was diluted in a 5 ml vessel with a saturated ASA-EtOH solution, which was infused by a gear pump with a pump rate of about 100 ml min^{-1} .

In experiment 2 product crystals were pumped from vessel I ($V_{\text{Vessel1}}=5 \text{ ml}$) to vessel II ($V_{\text{Vessel2}}=5 \text{ ml}$) with a pump rate of 6 ml min^{-1} . Subsequently saturated ASA-EtOH was infused into vessel II through the gear pump with a pump rate of 60 ml min^{-1} .

Figure 21 and Table 5 show the results of both experiments.

Setup determination for feedback control loop

The impact of the flow rates to the CSD were discussed in Eder et al. [13] [14] where the results show a nearly linear dependency of the average diameter size on the flow rate. In this work, the dependency will be referred to as response function henceforth. Based on

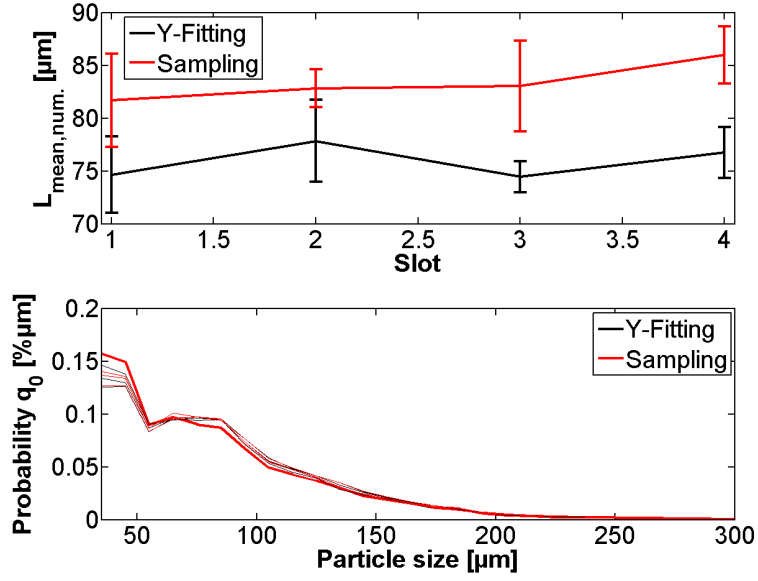


Figure 21: Mean product crystal size and CSD regarding the dilution method investigated *Top*: Mean product crystal size with error bars which denote the standard deviation $\sigma(L_{\text{mean},q_0})$ for a slot; *Bottom*: CSD of product crystal

Table 5: Measured mean crystal size with the corresponding standard deviation for a duration of 4 slots (i.e. about 45 min)

Slot	$L_{\text{mean},q_0(\text{Y-fit})} [\mu\text{m}]$	$\sigma_{q_0(\text{Y-fit})} [\mu\text{m}]$	$L_{\text{mean},q_0(\text{Pump})} [\mu\text{m}]$	$\sigma_{q_0(\text{Pump})} [\mu\text{m}]$
1	74.64	3.63	81.68	4.39
2	77.84	3.89	82.81	1.79
3	74.45	1.49	83.04	4.29
4	76.74	2.42	85.97	2.70

the influence of the feed and seed concentration on the final product crystal size, three different settings ($c_{\text{feed sol.}}$ & $c_{\text{seed susp.}}$) were tested to determine an appropriate process set-up for the implementation of the feedback control.

The concentration settings used for the feed solution $c_{\text{feed sol.}}$ and the seed suspension $c_{\text{seed susp.}}$, the adjusted seed pump rates V_{seed} and the temperature of each temperature bath ($T_{\text{feed sol.}}$, $T_{\text{B1-B3}}$) for each setting are shown in Table 6. Figure 22 presents the mean product crystal size with the seed pump rate adjusted for each setting investigated.

Table 6: Investigated process settings with used pump rates

Setting	$c_{\text{feed sol.}}$	$c_{\text{seed susp.}}$	$T_{\text{feed sol.}}$ [°]	$T_{\text{B1}}/T_{\text{B2}}/T_{\text{B3}}$ [°]	V_{seed} [ml min ⁻¹]
1	0.40	0.30	36	29/25/22	4/6/8/10
2	0.45	0.30	34	28/25/22	3/4/6/8/10
3	0.45	0.40	34	28/25/22	3/4/5/6/8/10

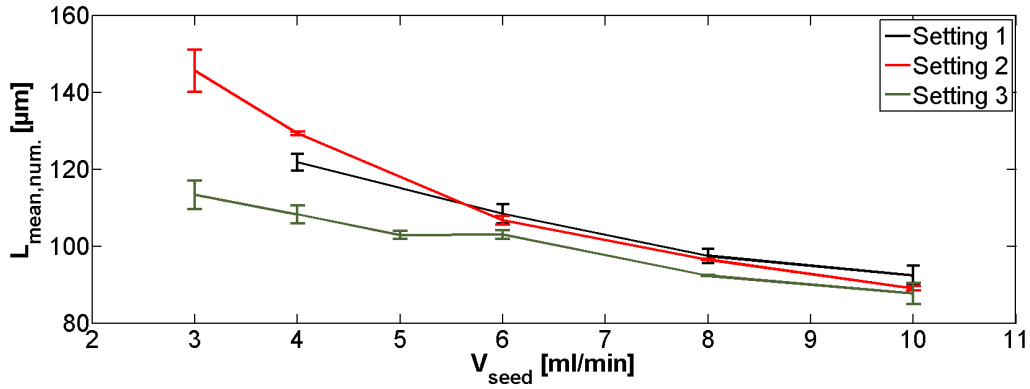


Figure 22: Response function of the three process settings in Table 6

3.6.2 Control

An ASA-EtOH feed solution (Feed sol.) with a concentration of $c_{\text{feed sol.}} = 0.45 \text{ g}_{\text{ASA}} \text{ g}_{\text{EtOH}}^{-1}$ was kept at around $40 \pm 0.2 \text{ }^\circ\text{C}$ in its storage vessel to guarantee complete solubility, whereas the ASA-EtOH seed suspension (Seed susp.), generated as described above, was stirred at $22 \pm 0.2 \text{ }^\circ\text{C}$. Peristaltic pumps fed the solution (PI) and the suspension (PII) via a Y-fitting into the crystallizer. Before entering the Y-fitting, a thermostatic bath was employed to bring the feed solution to $40 \pm 0.2 \text{ }^\circ\text{C}$. The crystallizer itself consisted of a 15 m tube cooled subsequently by three thermostatic bathes (BI: $29 \text{ }^\circ\text{C}$, BII: $25 \text{ }^\circ\text{C}$, BIII: $22 \text{ }^\circ\text{C}$). The supersaturation after the Y-fitting is determined by the concentration of the feed solution, the feed and seed pump rates V_{feed} & V_{seed} as well as their temperatures T_{feed} & T_{seed} . The latter should be tuned in a way that a slightly supersaturated feed stream enters the crystallizer so as not to dissolve seed crystals.

After the product slurry had exited the tubular crystallizer samples were withdrawn (V_{CSD}) for CSD analysis. Before entering the measuring chamber, the withdrawn slurry was diluted with a saturated solution ($V_{\text{sat.}}$) to prevent more than one particle to pass the measuring chamber simultaneously. For each CSD measurement, the diluted product slurry was pumped through the CSD analyzer ($V_{\text{anal.}}$) for 30 s. Subsequently, the measuring cell was rinsed with EtOH for 40 s. Within each slot the CSD was determined at least in triplicate. A list about the used process settings is shown in Table 7.

Table 7: Process settings for the ASA-Crystallization

Symbol	Description	Value
$c_{\text{feed sol.}}$	ASA concentration feed solution	$0.45 \text{ g}_{\text{ASA}} \text{ g}_{\text{EtOH}}^{-1}$
$c_{\text{seed susp.}}$	ASA concentration seed suspension	$0.30 \text{ g}_{\text{ASA}} \text{ g}_{\text{EtOH}}^{-1}$
$T_{\text{feed sol.}}$	Temperature feed solution	$36 \text{ }^\circ\text{C}$
$T_{\text{seed susp.}}$	Temperature seed suspension	$22 \text{ }^\circ\text{C}$
$T_{\text{Bath 1}}$	Temperature of thermostatic bath 1	$29 \text{ }^\circ\text{C}$
$T_{\text{Bath 2}}$	Temperature of thermostatic bath 2	$25 \text{ }^\circ\text{C}$
$T_{\text{Bath 3}}$	Temperature of thermostatic bath 3	$22 \text{ }^\circ\text{C}$
$V_{\text{feed sol.}}$	Pump rate feed solution	20 ml min^{-1}
$V_{\text{seed susp.}}$	Pump rate seed suspension	6 ml min^{-1}
V_{CSD}	Pump rate of product crystals to detector	20 ml min^{-1}
$V_{\text{sat.}}$	Pump rate saturated solution	50 ml min^{-1} – 60 ml min^{-1}

4 Experimental results

4.1 Consistency of the tubular crystallizer

Before applying feedback control, the presented process set-up was tested with regard to the CSD consistency. Therefore, the tubular crystallizer was operated for one hour, i.e., five slots, using the process settings listed in Table 7 and a single seed-batch. The CSD measurements are shown in Figure 23. Table 8 shows the mean product crystal size L_{mean,q_0} for each slot with the corresponding standard deviation σ_{q_0} . In addition, the pressure within the crystallizer was recorded during the experiment (see Figure 24).

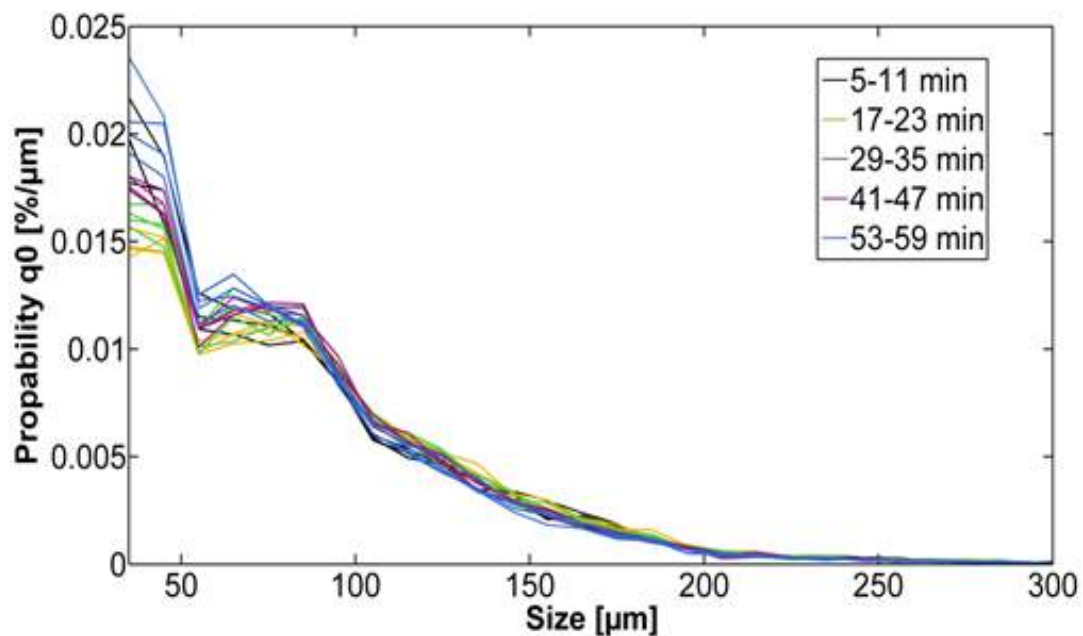


Figure 23: CSD measurements of the consistency experiment with a duration of 59 min

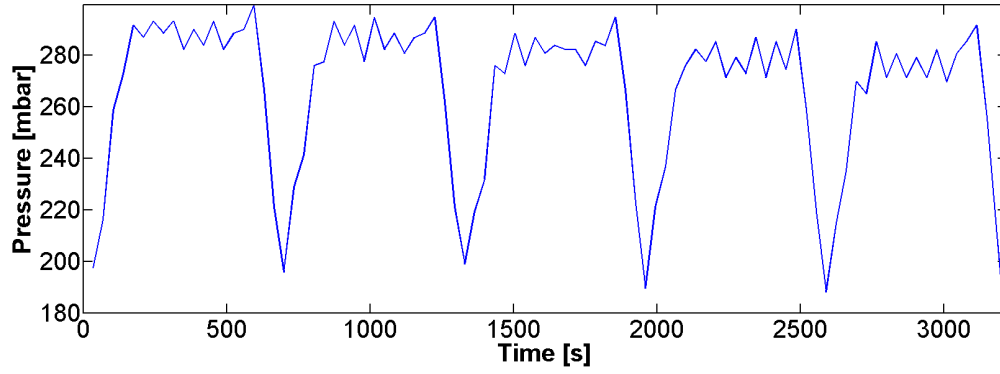


Figure 24: Pressure within the crystallizer for 5 slots (i.e. a duration of about 55 min)

Table 8: Mean product crystal size $L_{\text{mean},q0}$ with the standard deviations σ_{q0} for a slot

Slot	$L_{\text{mean},q0}$ [μm]	σ_{q0} [μm]
1	85.04	4.66
2	87.15	0.71
3	84.87	1.48
4	82.97	0.67
5	79.78	1.65

4.2 Tuning the mean crystal size to 140 μm

Figure 25 shows the results of two control experiments with the objective to tune $L_{\text{mean},q0}$ to 140 μm . For both experiments, the tubular crystallizer was initially operated using the settings listed in Table 7, i.e., a seed suspension pump rate of 6 ml min^{-1} . The discrepancy between both experiments originates from different seedings as shown in Figure 27 a/b. An ultrasound irradiation time of 70 s was used for the seed-batch of experiment 1 whereas an irradiation time of 60 s was used for the seed-batch of experiment 2. Hence, the seeds used for experiment 2 were smaller. The CSDs of the product crystals are shown at the bottom of Figure 25. In addition, the pressure for both experiments is shown in Figure 26.

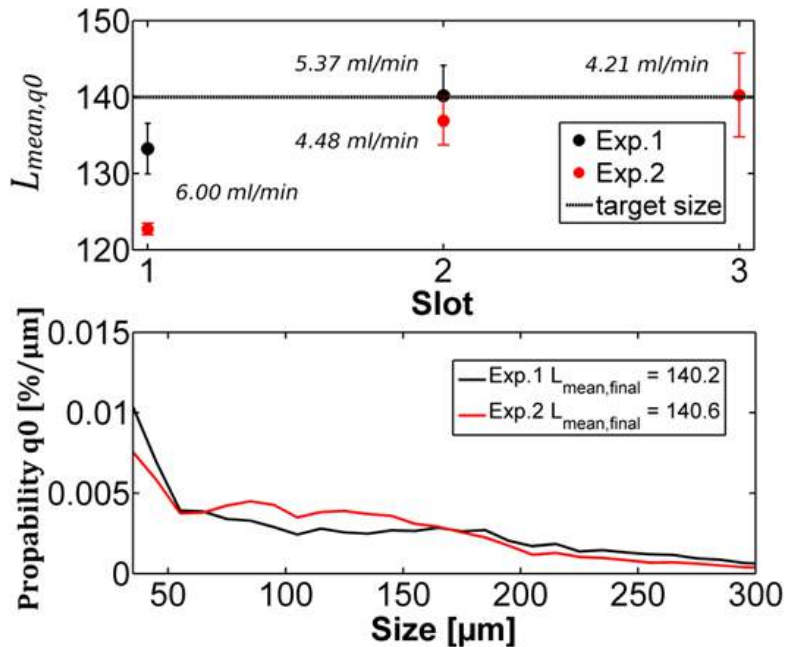


Figure 25: Tuning the mean crystal size value to 140 μm in two experiments *Top*: Change of mean crystal size from slot to slot The current seed suspension pump rates are inserted and the error bars denote the standard deviations $\sigma(L_{\text{mean},q0})$ for a slot *Bottom*: CSD of the tuned product crystals

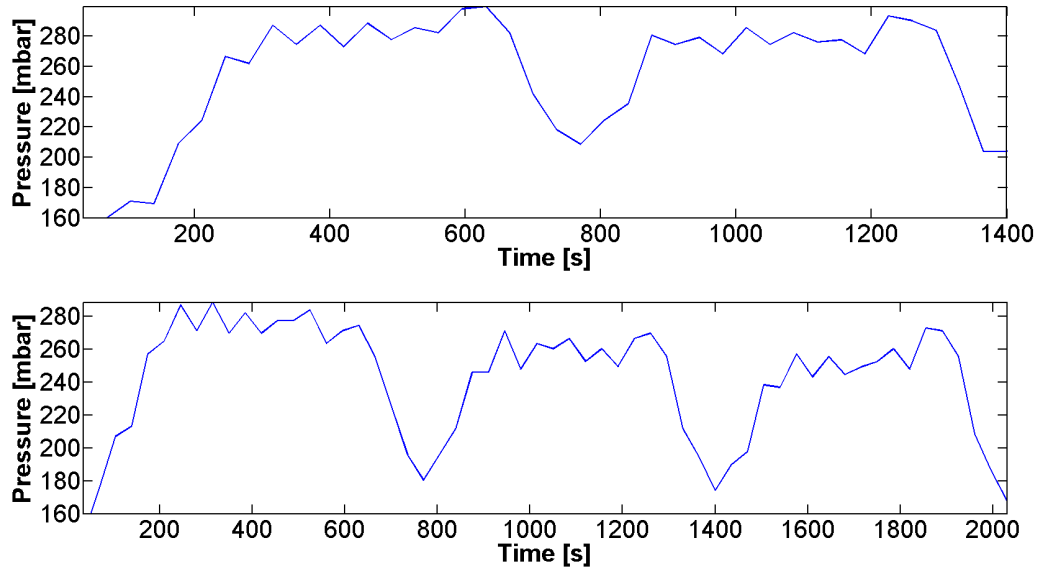


Figure 26: Pressure within the crystallizer during the feedback control tuning product crystals to a size of $140\ \mu\text{m}$ using two different seed batches *Top*: Experiment1 *Bottom*: Experiment2

Table 9: Control history of tuning the mean product crystals to $140\ \mu\text{m}$ for two different seed batches

Experiment	$L_{\text{mean},q0}$ measured [μm]	$V_{\text{seed } i}$ [ml min^{-1}]	$V_{\text{seed } i+1}$ [ml min^{-1}]	ϵ [μm]
1	133.23	6	5.37	-6.77
	140.17	5.37	5.40	0.17
2	122.73	6	4.48	-17.27
	136.92	4.48	4.21	-3.08
	141.11	4.21	4.32	1.11

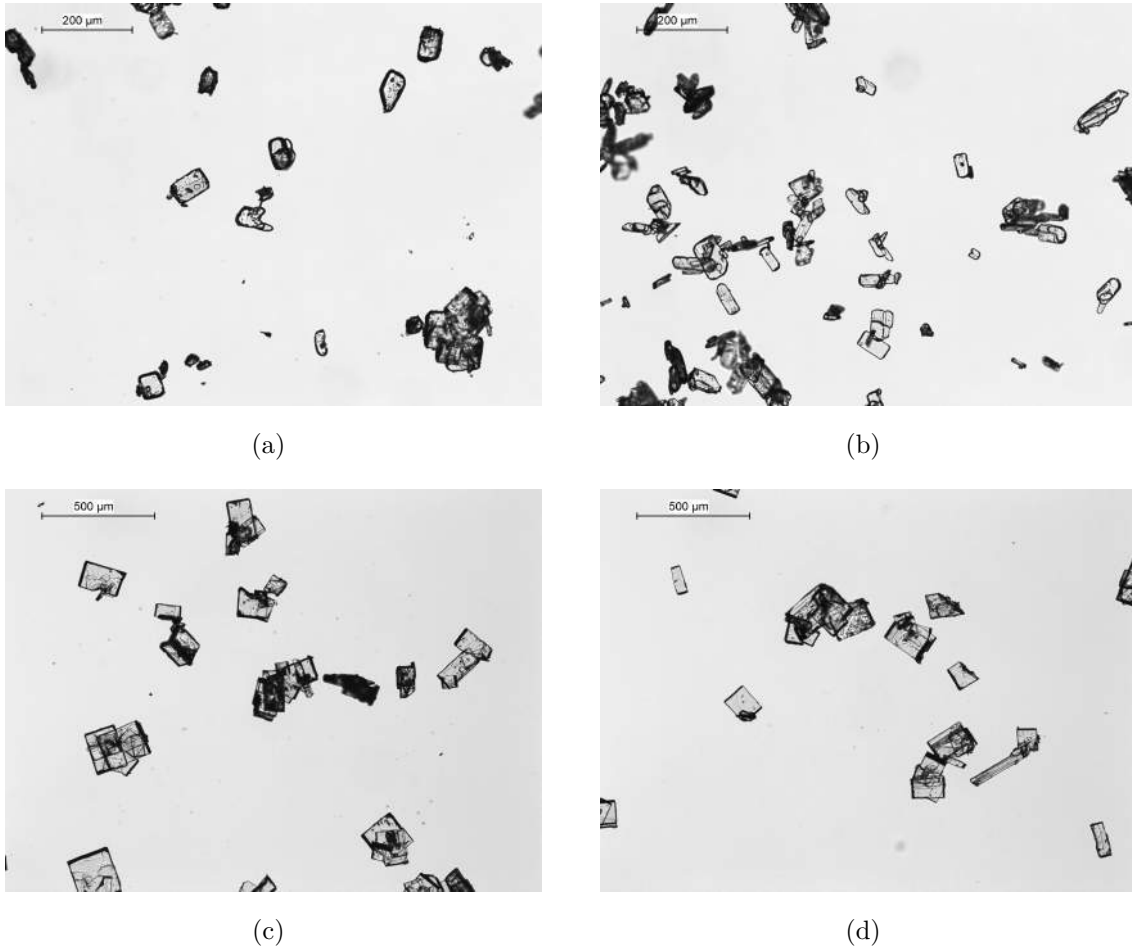


Figure 27: Micrographs with two different magnifications of: a) Seeds Exp.1; b) Seeds Exp.2; c) Product crystals Exp.1; d) Product crystals Exp.2

4.3 Stepwise tuning of the mean crystal size

In order to further examine the feedback control loop, the mean crystal size was tuned to four target values decreasing subsequently by $10\ \mu\text{m}$ starting from $130\ \mu\text{m}$ (i.e., $130\ \mu\text{m}$, $120\ \mu\text{m}$, $110\ \mu\text{m}$, $100\ \mu\text{m}$, $90\ \mu\text{m}$). The CSD of the successfully tuned product crystals and the control history, i.e., how $L_{\text{mean},q0}$ changes from slot to slot, are presented in Figure 28. Table 10 comprises the tuned product mean crystal size $L_{\text{mean},q0}$, the current seed pump rate $V_{\text{seed } i}$, the calculated pump rate $V_{\text{seed } i+1}$ and the deviation ϵ of the product mean crystal size from the target size.

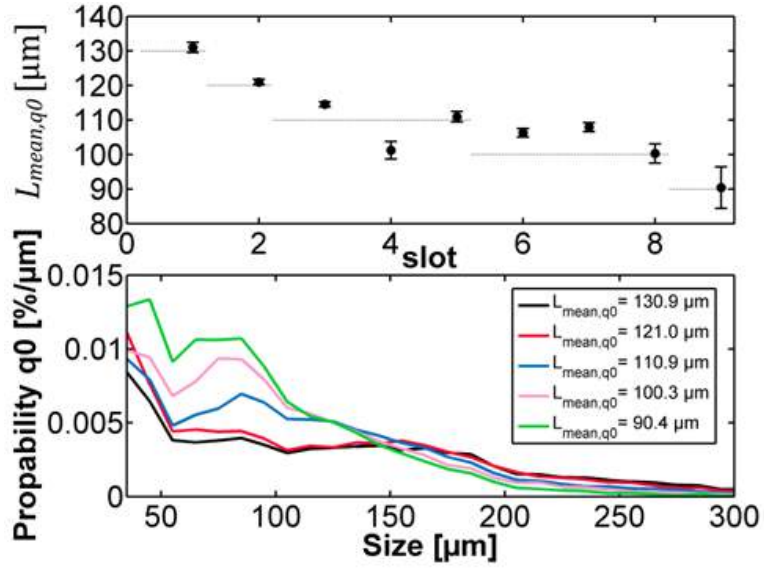


Figure 28: Stepwise control of the mean crystal size: $130\ \mu\text{m} \rightarrow 120\ \mu\text{m} \rightarrow 110\ \mu\text{m} \rightarrow 100\ \mu\text{m} \rightarrow 90\ \mu\text{m}$. *Top*: Control history, the error bars denote the standard deviations $\sigma(L_{\text{mean},q0})$ for a slot. *Bottom*: CSD of the tuned product crystals

Table 10: Control history of the stepwise control of the mean crystal size including the target size $L_{\text{mean},q0\ \text{target}}$, the size measured $L_{\text{mean},q0\ \text{measured}}$, the current pump rate $V_{\text{seed } i}$, the pump rate calculated $V_{\text{seed } i+1}$ and the deviation ϵ between target and measured size.

$L_{\text{mean},q0\ \text{target}}\ [\mu\text{m}]$	$L_{\text{mean},q0\ \text{measured}}\ [\mu\text{m}]$	$V_{\text{seed } i}\ [\text{ml min}^{-1}]$	$V_{\text{seed } i+1}\ [\text{ml min}^{-1}]$	$\epsilon\ [\mu\text{m}]$
130	130.96	4	4.99	0.96
120	120.97	4.99	5.56	0.97
110	114.31	5.56	5.95	4.31
	101.49	5.95	5.20	-8.51
	110.95	5.20	6.33	0.95
100	106.27	6.33	7.13	6.27
	107.90	7.13	8.21	7.90
	100.30	8.21	11.07	0.30
90	90.40	11.07	14.00	0.40

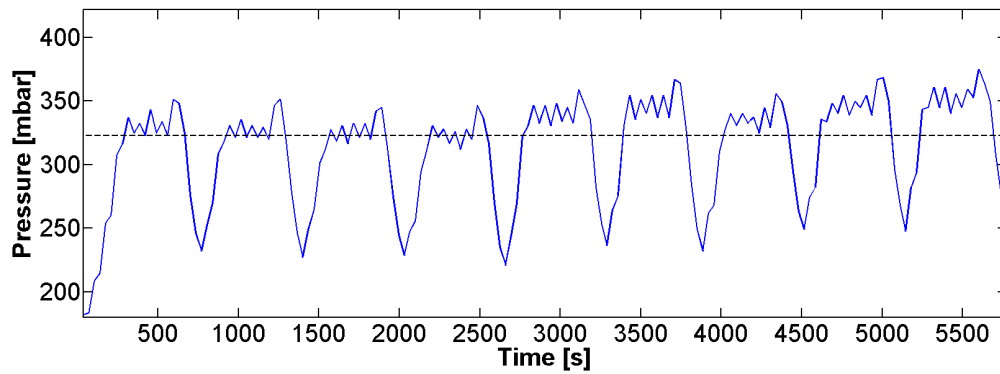
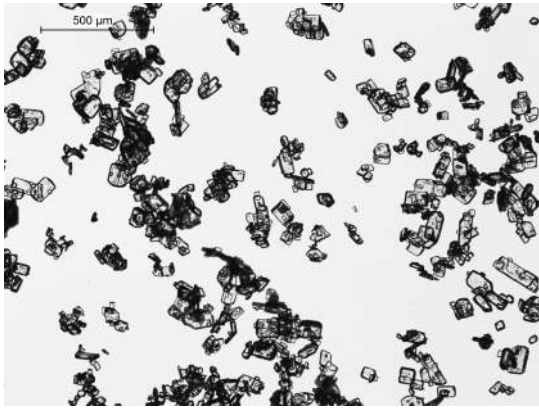
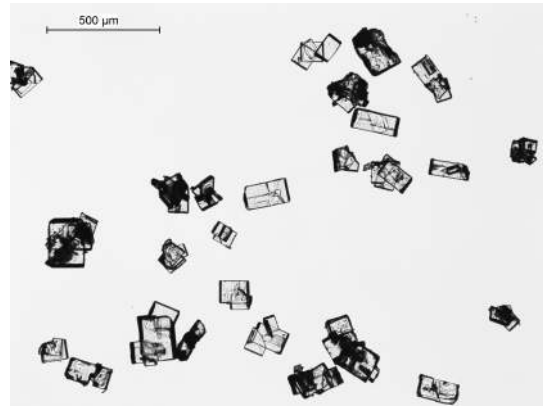


Figure 29: Pressure of the stepwise tuning of the product crystal size during an experimental time of 9 slots (i.e. a duration of about 95 min)

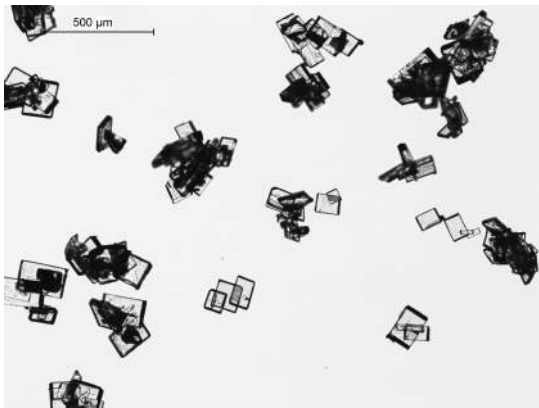
In consideration of a possible change of the pressure in parallel to the product mean crystal size, the pressure within the tubular reactor is presented in Figure 29. Micrographs of the product crystals are presented in Figure 30.



(a)



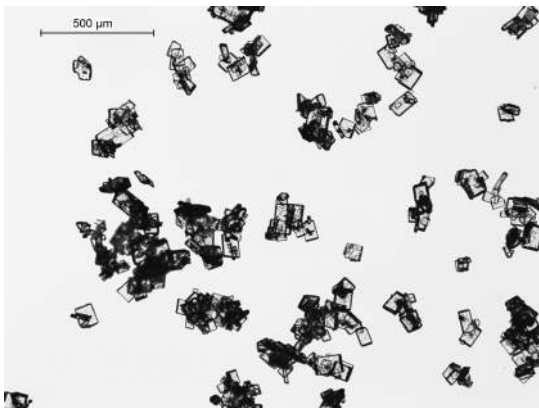
(b)



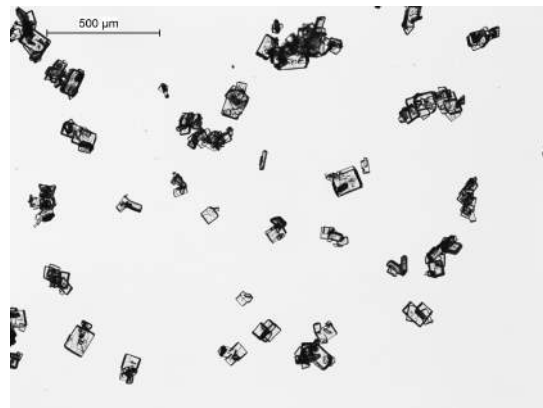
(c)



(d)



(e)



(f)

Figure 30: Micrographs of Seed/product crystals a) Seed Crystals b)130 μm c)120 μm d)110 μm e)100 μm f)90 μm

5 Discussion

5.1 Hardware and setup

This chapter describes the considerations behind the hardware technical part and the used setup of this master thesis in a critical way.

Particle measurement

The integration of the feedback control loop into an existing tubular crystallizer required the implementation of an online particle measurement system. Therefore a particle counter, based on a light extinction principle, was chosen as an appropriate measurement device for the continuous measurement of the particle size.

Valve control

In respect of the control of the valve system and the pressure sensor, the Arduino Uno board was an appropriate control unit due to the easy implementation and its support for MATLAB. An additional feature was the possible control of each individual valve via the given input/output pins of the micro-controller. To protect the I/O pins of the micro-controller against overvoltage, relay boards were implemented between the Arduino Uno board and the power supply of each valve.

Valves

At the beginning of the hardware development, magnetic valves were used for the sampling of product crystals and passing them to the particle counter. Due to sedimentation of the product crystals, which resulted in an accumulation of particles within the valve, the magnetic valve for sampling was exchanged for a tube pitch valve. Due to a high operating temperature of the magnetic valves, the power supply was decreased by a buck

converter from 24 V to 12 V. Initial measurements showed that by changing the power supply to 12 V the temperature of the solution remained constant along the valve.

Dilution

By diluting product crystals with a saturated ASA-EtOH solution, the measurement of overlapping particles within the measuring chamber of the particle counter was avoided which prevented erroneous CSD measurements of the product crystals. Based on the work of Eder et al.[13] [14] an approximate mean product crystal size of 150 μm was expected. Thus, regarding the calculation in chapter 3.3.2 an eightfold dilution was required at least. Due to the high consumption of saturated ASA-EtOH solution for dilution, various methods for the dilution process were investigated so as to find out the most efficient one.

As an example, for an overall process stream of 26 ml min^{-1} the required pump rate for the dilution with saturated ASA-EtOH has to be at least 208 ml min^{-1} in case of the direct dilution of the process stream. Keeping in mind, that experiments with the feedback controller last for 45 min–90 min, a total volume of 9 l–19 l of saturated ASA-EtOH would be required. In contrast, by sampling only parts of the process stream, the required amount of saturated ASA-EtOH for dilution would be automatically decreased. Assuming that parts of the process stream are sampled with a pump rate of 6 ml min^{-1} , the required pump rate for the dilution has to be at least 48 ml min^{-1} . As a result the amount of saturated ASA-EtOH is reduced to 160 ml min^{-1} .

Therefore initial studies for the choice of the dilution method were conducted. The consistency of two different dilution methods was investigated in two experiments which are described in chapter 3.6.1.

Figure 21 shows the consistency of the measured product crystals for both dilution methods. Table 5 comprises the data of both dilution experiments, including the mean product crystal size ($L_{\text{mean},q0(\text{Y-fit})}$, $L_{\text{mean},q0(\text{Pump})}$) and the corresponding deviation for a slot ($\sigma_{q0(\text{Y-fit})}$, $\sigma_{q0(\text{Pump})}$). Both investigated dilution methods show deviations of the mean product crystal size lower than 5 μm which indicates the equivalence of both investigated methods.

The variance of the measured CSD indicates the sensitivity of the crystallization process to the minimal change of process conditions (e.g. temperature, pump rates, etc.).

In comparison to the implementation of a Y-fitting, the dilution via an additional pump showed advantages which are:

- a known mass flow of particles (pump rate from vessel 1 into vessel 2 is 6 ml min^{-1})
- the pump rate for the saturated ASA-EtOH solution can be set to a constant value
- experiments are reproducible
- less consumption of saturated ASA-EtOH solution compared to the Y-fitting method

In contrast to the aforementioned advantages, the final size of the product crystals may be influenced by additional parameters. For example, with the increased distance between the crystallizer and the particle counter, an extended residence time of the product crystals is created which can result in a change of the crystal size. In addition, mechanical forces caused by the stirrer in vessel 1 respectively vessel 2 or by the peristaltic pump can induce breakages which again change the resulting final product crystal size.

Nonetheless, the setup for the dilution method with the additional pump was further used for the implementation of the feedback control loop system due to the aforementioned advantages.

Determination of an appropriate setup

The strategy behind the feedback control loop was the calculation of a new seed pump rate based on the size deviation ϵ between the measured mean product crystal size $L_{\text{mean},q0 \text{ measured}}$ and the desired mean product crystal size $L_{\text{mean},q0 \text{ target}}$. Thereby, a generic response function was defined in order to calculate the necessary change of the seed pump rate to achieve the target product crystal size. For the determination of an appropriate set-up various process settings were investigated which are described in chapter 3.6.1.

The level of supersaturation after the first Y-fitting is determined by the interplay between the feed solution's and seed suspension's pump rate and their temperatures and needs to be kept slightly above one (i.e., supersaturated). Regarding the different concentration of the feed solution and seed suspension for each investigated setting (see Table 6), respectively, the temperature of each temperature bath had to be adapted. There-

fore calculations for the necessary temperature were conducted based on the model of Besenhard et al. [49].

For the tested setting 1 and 3 an almost linear relation between the mean product crystal size and the seed pump rate was observed in Figure 22. In contrary, the results of setting 2 show a non-linear increase of the particle size in relation to a decreasing seed pump rate. Despite the non-linear behavior, setting 2 was used for the development of the feedback controller.

Due to plugging of the crystallizer, the measurement of some data points was not possible (e.g. mean product crystal size for a seed pump rate of 3 and 5 ml min⁻¹ for process setting 1).

5.2 Software

As mentioned in chapter 3.4 three tasks were executed in parallel which were the measurement of the CSD:

- the control of the valve system
- the data acquisition
- the evaluation and control

Each individual task will be discussed hereafter.

CSD Measurement

The software "Protrend" provided together with the particle counter was used to conduct the measurement of the product crystals. In respect of an optimization of the software design in this work (see chapter 3.4), the control of the particle counter via MATLAB would provide advantages in respect of the measurement procedure. Due to a possible high effort for the development of a MATLAB interface, CSD measurements were taken with the Protrend software.

Valve control

In respect of the necessary time to evaluate the measured CSD data and the subsequent response of the feedback controller, the tasks for the valve control and the data processing, respectively, had to be established in parallel. Thus, to ensure an autonomous measurement process structure both tasks were implemented separately. The communication between the control and data processing unit were conducted by the export of the status variable `status_val_pro`.

For monitoring purposes, the pressure within the crystallizer was measured at each switch of the valves.

Data acquisition/evaluation and control

As mentioned in chapter 3.4.3 the consistency of the measured CSD was determined by the implementation of three individual test cases.

The threshold value for the chi-test was obtained solely from initial studies during the development of the feedback loop system. Since the log-normal distribution is a commonly used distribution function for the approximation of a measured CSD [39], equation 17 is expected to give higher values in the presence of outliers and measurement errors.

One critical point of the consistency tests was the fact that the last three measurements within a slot were taken as test reference. Due to the high sensitivity of the crystallizer and the dilution method, possible deviations in the results of the taken CSD measurements were possible. Depending on the settings used for the consistency test (e.g. threshold of the mean value) CSD measurements were discarded, even if the measurement had been correct. Due to the short steady state window in each slot, it was possible that two slots were necessary in order to change the control variable (e.g. seed pump rate).

5.3 Experimental results

5.3.1 Consistency of the tubular crystallizer

The results in Figure 23 show apparently no trend in the CSD, neither to bigger nor smaller product crystals. Over the entire run deviations in $L_{\text{mean},q0}$ are in a range of 8 μm . Parallel to the measured CSD, the obtained pressure data in Figure 24 demonstrates a similar tendency. The pressure fluctuated only within a range of 3 mbar. Both results indicate that process conditions which affect the CSD (e.g. pump rates, temperatures and the seed loading i.e., the solid mass fraction of the fed seed suspension) vary only within an acceptable range. Hence we assume that the presented set-up is suitable to monitor and control the mean crystal size.

5.3.2 Tuning the mean crystal size to 140 μm

Figure 25 shows the results of two control experiments using different seed-batches with the objective to tune $L_{\text{mean},q0}$ to 140 μm . The pressure varied between 278 mbar–281 mbar during experiment 1 (Exp.1) and between 270 mbar–263 mbar during experiment 2 (Exp.2).

Regarding the results of both experiments (see Table 9), it was demonstrated that even for seed crystals of different sizes, the feed back control was able to manage and regulate the control variable (e.g. the seed pump rate), for the precise production of particles of the target size within a range of 1 μm . By using the feedback control it was possible to achieve the target mean crystal size after just one manipulation of V_{seed} (one more slot) in the case of experiment 1 and two manipulations (2 more slots) in the case of experiment 2.

As expected from the shorter irradiation time, seed micrographs (see Figure 27a/b) indicate that the seeds of experiment 2 were bigger and had less fines (crystals < 10 μm) compared to the seeds used in experiment 1. Hence, experiment 2 is expected to yield bigger product crystal using identical settings and requires a higher final seed pump rate assuming that the crystal size changes only via growth. This is in conflict with the

experimental observations which indicate an additional mechanism that alters the CSD. It is known that the likelihood of aggregation (and agglomeration) events is higher if the crystals are smaller [53]. Since the experiment with smaller seeds obtained larger product crystals, a considerable amount of aggregation events seems plausible.

5.3.3 Stepwise tuning of the mean crystal size

While the target mean crystal size of the first two steps (130 μm & 120 μm) was accomplished with the aid of one V_{seed} manipulation the following steps (110 μm & 100 μm) required three slots each. The last tuning step (100 μm) was again accomplished via a single V_{seed} manipulation.

Starting with a value of 4 ml min^{-1} the controller calculated and adjusted an appropriate seed pump rate $V_{\text{seed } i+1}$ for each step to achieve the desired particle size $L_{\text{mean},q0 \text{ target}}$ (see Table 10). A new target size was set in the MATLAB command prompt after the result of the CSD measurement had been successfully tuned to the desired size. The feedback controller worked for positive as well as for negative error values (ϵ) which demonstrates the capability of the controller to manage and regulate the control variable (seed pump rate) for particles, bigger and smaller, than the target particle size respectively.

Beginning with a pressure value of 330 mbar for a product crystal size of 130 μm , the pressure increased about 10 mbar–20 mbar when particles of the size of 110 μm and smaller were taken from the crystallizer. This increase is expected due to increase of the seed pump rate.

Due to the limiting volume of the vessels used for the feed solution (Feed vessel: 1 l) and seed suspension (Seed vessel: 0.5 l), respectively, the experiment had to be restarted with a new seed and feed batch. Both batches were made in the same way as the seed and feed batch at the beginning of the experiment. The experiment was restarted beginning from the last target particle size of 110 μm .

5.4 Optimization

During the development process of the feedback control loop, improvements in the hardware and software technical part of this work were taken into consideration which may facilitate the crystallization process and the feedback control, respectively.

The production of crystals of more than 160 μm was not possible with the process set-up used. Tube plugging was observed when crystal sizes above 160 μm were produced. In addition, plugging also occurred at critical points of the crystallizer (e.g. transitions from one temperature bath to another). Thus, for further experiments, tubes with a bigger inner diameter than 2 mm may improve the crystallizer in respect of the stability during the crystallization process and the production of product crystals bigger than 160 μm , respectively.

Referring to the equipment used in this work, the accuracy and consistency of the peristaltic pumps has to be considered. Due to the attrition of the tubing in the peristaltic pump, the pump rate may have varied with time. Thus, the implementation of a flow sensor may help to monitor the current pump rate of the peristaltic pump. In addition, the control of the particle counter via MATLAB would facilitate the measurement procedure. For example the experimental time could be decreased and thus the required amount of the model substances (seed suspension, feed solution, saturated ASA-EtOH for dilution) used.

5.5 Conclusion

The implementation of a feedback control loop for a continuous tubular crystallizer was conducted in this work. The principle of seeded crystallization was realized in a tubular crystallizer with an inner diameter of 2 mm. Acetylsalicylic acid (ASA) and ethanol (EtOH) were used as model substances. The generation of ASA-Seeds in EtOH-ASA was conducted via sonocrystallization. Under controlled conditions (e.g. temperature) the seed suspension was fed into the crystallizer and mixed with a slightly undersaturated EtOH-ASA feed solution. Subsequently the product crystals were measured online via a particle counter. In order to measure the crystal size distribution of the manufactured

particles, the suspension of product crystals was diluted with a saturated EtOH-ASA solution. Due to encrusting within the crystallizer which provoke tube plugging, the tubular reactor was rinsed with pure EtOH at a regular interval of 7 min. To ensure the consistency of the measured CSD within a slot, test methods were implemented which discarded erroneous CSD measurements. A simple controller was developed based on the response function which was defined in order to adjust the control variable according to the deviation of the measured and target crystal size. The response function was obtained solely from experiments.

This work mainly focuses on the proof of concept for the realization of a feedback control loop for a continuous tubular crystallizer. It was shown that with an appropriate design, hardware and process environment the reproduction of a certain particle size was feasible. The controller provides the possibility of producing crystal particles of a desired mean product crystal size within a range of 3 μm . A measurement system was implemented which provides the possibility to monitor the crystal size distribution of the produced crystal particles.

Three experiments were conducted to demonstrate the performance of the feedback controller implemented which are

- The consistency of the production of crystals was tested over a process duration of about 60 min. The results show that over the entire run a deviation in the measured mean particle size is in the range of 8 μm . Thus the consistency was proven for an acceptable range.
- Starting with seed suspensions of different sizes, the controller managed the production of crystal product in the size of 140 μm . The target size was reached for both seed suspensions used. Therefore, it was shown that the initial seed size is not a parameter required for the final product crystal size.
- It is shown that the production of crystals of various sizes is possible.

Besides a proof of concept for the feedback controller, the results of this work can be summarized as follows

- An ultrasound-assisted seed generation method was presented, capable of producing small seed crystals with a narrow CSD and a low amount of fines.

- Pressure recordings indicate that the percentage of solid material in the tubing as well as the particle size can be estimated via a pressure probe.
- A cleaning concept for the tubular crystallizer is presented which enables long term runs. A consistency study demonstrates that the product's CSD is maintained accurately if the process settings are kept constant.
- Aggregation is expected to occur if the seed pump rate undercuts a threshold value (\approx) 4.5 ml min^{-1} using the process settings in Table 7. Crystal size tuning was also possible in the presence of aggregation. Nevertheless, the obtained CSDs were less consistent

In summary, the results of our study demonstrate the potential for highly accurate crystal size tuning in a tubular crystallizer via a simple feedback control strategy. Only a few experiments are required to set up a controller due to the simple design of the presented crystallizer.

Bibliography

- [1] MULLIN, J.W.: *Crystallization*. Butterworth-Heinemann, 1993
- [2] ALVAREZ, Alejandro J. ; MYERSON, Allan S.: Continuous plug flow crystallization of pharmaceutical compounds. In: *Crystal Growth & Design* 10 (2010), Nr. 5, S. 2219–2228
- [3] OULLION, M ; PUEL, F ; FÉVOTTE, G ; RIGHINI, S ; CARVIN, P: Industrial batch crystallization of a plate-like organic product. In situ monitoring and 2D-CSD modelling: Part 1: Experimental study. In: *Chemical Engineering Science* 62 (2007), Nr. 3, S. 820–832
- [4] OULLION, M ; PUEL, F ; FEVOTTE, G ; RIGHINI, S ; CARVIN, P: Industrial batch crystallization of a plate-like organic product. In situ monitoring and 2D-CSD modelling. Part 2: Kinetic modelling and identification. In: *Chemical engineering science* 62 (2007), Nr. 3, S. 833–845
- [5] SHEKUNOV, Boris Y. ; CHATTOPADHYAY, Pratibhash ; TONG, Henry H. ; CHOW, Albert H.: Particle size analysis in pharmaceuticals: principles, methods and applications. In: *Pharmaceutical research* 24 (2007), Nr. 2, S. 203–227
- [6] SARKAR, Debasis ; ROHANI, Sohrab ; JUTAN, Arthur: Multi-objective optimization of seeded batch crystallization processes. In: *Chemical Engineering Science* 61 (2006), Nr. 16, S. 5282–5295
- [7] GROS, Håkan ; KILPIÖ, Teuvo ; NURMI, Juha: Continuous cooling crystallization from solution. In: *Powder technology* 121 (2001), Nr. 1, S. 106–115
- [8] VARIANKAVAL, Narayan ; COTE, Aaron S. ; DOHERTY, Michael F.: From form to

- function: Crystallization of active pharmaceutical ingredients. In: *AIChE journal* 54 (2008), Nr. 7, S. 1682–1688
- [9] FUTRAN, Mauricio ; HSU, Jaanpyng ; LIU, Paul D. ; MIDLER JR, Michael ; PAN, Shih-Hsie ; PAUL, Edward L. ; WHITTINGTON, Edwin F.: *Crystallization method to improve crystal structure and size*. Mai 24 1994. – US Patent 5,314,506
- [10] AM ENDE, David ; BRENEK, Steven: *Crystallization method and apparatus using an impinging plate assembly*. 2003
- [11] SCHIEWE, Joerg ; ZIERENBERG, Bernd: *Process and apparatus for producing inhalable medicaments*. 2003
- [12] RÍO, José R. ; ROUSSEAU, Ronald W.: Batch and tubular-batch crystallization of paracetamol: crystal size distribution and polymorph formation. In: *Crystal growth & design* 6 (2006), Nr. 6, S. 1407–1414
- [13] EDER, Rafael J. ; RADL, Stefan ; SCHMITT, Elisabeth ; INNERHOFER, Sabine ; MAIER, Markus ; GRUBER-WOELFLER, Heidrun ; KHINAST, Johannes G.: Continuously seeded, continuously operated tubular crystallizer for the production of active pharmaceutical ingredients. In: *Crystal Growth & Design* 10 (2010), Nr. 5, S. 2247–2257
- [14] EDER, RJP ; SCHMITT, EK ; GRILL, J ; RADL, S ; GRUBER-WOELFLER, H ; KHINAST, JG: Seed loading effects on the mean crystal size of acetylsalicylic acid in a continuous-flow crystallization device. In: *Crystal Research and Technology* 46 (2011), Nr. 3, S. 227–237
- [15] EDER, Rafael J. ; SCHRANK, Simone ; BESENHARD, Maximilian O. ; ROBLEGG, Eva ; GRUBER-WOELFLER, Heidrun ; KHINAST, Johannes G.: Continuous sonocrystallization of acetylsalicylic acid (ASA): control of crystal size. In: *Crystal Growth & Design* 12 (2012), Nr. 10, S. 4733–4738
- [16] NAGY, Zoltan K. ; BRAATZ, Richard D.: Advances and New Directions in Crystallization Control. In: *Annual Review of Chemical and Biomolecular Engineering* 3 (2012), Nr. 1, S. 55–75

- [17] FUJIWARA, Mitsuko ; NAGY, Zoltan K. ; CHEW, Jie W. ; BRAATZ, Richard D.: First-principles and direct design approaches for the control of pharmaceutical crystallization. In: *Journal of Process Control* 15 (2005), S. 493–504
- [18] NAGY, Zoltan K. ; FEVOTTE, Gilles ; KRAMER, Herman ; SIMON, Levente L.: Recent advances in the monitoring, modelling and control of crystallization systems. In: *Chemical Engineering Research and Design* 91 (2013), S. 1903–1922
- [19] MESBAH, Ali ; KALBASENKA, Alex N. ; HUESMAN, Adrie E. ; KRAMER, Herman J. ; HOF, Paul M. d.: Real-time dynamic optimization of batch crystallization processes. In: *Proceedings of the 17th IFAC World Congress, Seoul, Korea, 2008*, S. 3246–3251
- [20] CHIANESE, A. ; KRAMER, H. J.: *Industrial Crystallization Process Monitoring and Control*. Wiley, 2012
- [21] BAKAR, M. R A. ; NAGY, Zoltan K. ; RIELLY, Chris D.: Seeded batch cooling crystallization with temperature cycling for the control of size uniformity and polymorphic purity of sulfathiazole crystals. In: *Organic Process Research and Development* 13 (2009), S. 1343–1356
- [22] KEE, N C S. ; TAN, R B H. ; BRAATZ, R D.: Selective Crystallization of the Metastable α -Form of L-Glutamic Acid using Concentration Feedback Control. In: *Crystal Growth & Design* 9 (2009), S. 3044–3051
- [23] DOKI, Norihito ; SEKI, Hiroya ; TAKANO, Kiyoteru ; ASATANI, Haruki ; YOKOTA, Masaaki ; KUBOTA, Noriaki: Process control of seeded batch cooling crystallization of the metastable α -form glycine using an in-situ ATR-FTIR spectrometer and an in-situ FBRM particle counter. In: *Crystal Growth and Design* Bd. 4, 2004, S. 949–953
- [24] LIU, Jing J. ; HU, Yang D. ; WANG, Xue Z.: Optimization and control of crystal shape and size in protein crystallization process. In: *Computers & Chemical Engineering* 57 (2013), 133–140. <http://www.sciencedirect.com/science/article/pii/S0098135413001531>
- [25] VOLLMER, Ulrich ; RAISCH, Jörg: Control of batch crystallization-A system inver-

- sion approach. In: *Chemical Engineering and Processing: Process Intensification* 45 (2006), S. 874–885
- [26] ZHANG, K. ; NADRI, M. ; XU, C. Z.: Reachability-based feedback control of crystal size distribution in batch crystallization processes. In: *Journal of Process Control* 22 (2012), S. 1856–1864
- [27] SANG-IL KWON, Joseph ; NAYHOUSE, Michael ; ORKOULAS, Gerassimos ; CHRISTOFIDES, Panagiotis D.: Crystal shape and size control using a plug flow crystallization configuration. In: *Chemical Engineering Science* (2014)
- [28] SALEEMI, Ali N. ; STEELE, Gerry ; PEDGE, Nicholas I. ; FREEMAN, Anthony ; NAGY, Zoltan K.: Enhancing crystalline properties of a cardiovascular active pharmaceutical ingredient using a process analytical technology based crystallization feedback control strategy. In: *International Journal of Pharmaceutics* 430 (2012), S. 56–64
- [29] AAMIR, E. ; NAGY, Z. K. ; RIELLY, C. D.: Optimal seed recipe design for crystal size distribution control for batch cooling crystallisation processes. In: *Chemical Engineering Science* 65 (2010), S. 3602–3614
- [30] JIANG, Mo ; WONG, Min H. ; ZHU, Zhilong ; ZHANG, Jieqian ; ZHOU, Lifang ; WANG, Ke ; FORD VERSYPT, Ashlee N. ; SI, Tong ; HASENBERG, Lisa M. ; LI, Yao-En u. a.: Towards achieving a flattop crystal size distribution by continuous seeding and controlled growth. In: *Chemical Engineering Science* 77 (2012), S. 2–9
- [31] FERGUSON, Steven ; MORRIS, Gary ; HAO, Hongxun ; BARRETT, Mark ; GLENNON, Brian: Automated self seeding of batch crystallizations via plug flow seed generation. In: *Chemical Engineering Research and Design* (2014)
- [32] NAGY, Zoltan K. ; CHEW, Jia W. ; FUJIWARA, Mitsuko ; BRAATZ, Richard D.: Comparative performance of concentration and temperature controlled batch crystallizations. In: *Journal of Process Control* 18 (2008), S. 399–407
- [33] MAJUMDER, Aniruddha ; NAGY, Zoltan K.: Prediction and control of crystal shape distribution in the presence of crystal growth modifiers. In: *Chemical Engineering Science* 101 (2013), S. 593–602

- [34] DIRKSEN, JA ; RING, TA: Fundamentals of crystallization: kinetic effects on particle size distributions and morphology. In: *Chemical Engineering Science* 46 (1991), Nr. 10, S. 2389–2427
- [35] MULLIN, John W.: Crystallization and Precipitation. In: *Ullmann's Encyclopedia of Industrial Chemistry*. Wiley-VCH Verlag GmbH & Co. KGaA, 2000, S. 582–630
- [36] KORDYLLA, Anna ; KOCH, Stephan ; TUMAKAKA, Feely ; SCHEMBECKER, Gerhard: Towards an optimized crystallization with ultrasound: Effect of solvent properties and ultrasonic process parameters. In: *Journal of Crystal Growth* 310 (2008), S. 4177–4184
- [37] HEM, Stanley L.: The effect of ultrasonic vibrations on crystallization processes. In: *Ultrasonics* 5 (1967), Nr. 4, S. 202–207
- [38] ALLEN, T.: *Particle Size Measurement: Volume 1: Powder sampling and particle size measurement*. Springer, 1996
- [39] STIESS, Matthias: *Mechanische Verfahrenstechnik - Partikeltechnologie 1*. Springer, 2008
- [40] *A guidebook to particle size analysis*. http://www.horiba.com/fileadmin/uploads/Scientific/Documents/PSA/PSA_Guidebook.pdf
- [41] BURGESS, DianeJ. ; DUFFY, Eric ; ETZLER, Frank ; HICKEY, AnthonyJ.: Particle size analysis: AAPS workshop report, cosponsored by the Food and Drug Administration and the United States Pharmacopeia. In: *The AAPS Journal* 6 (2004), Nr. 3, S. 23–34
- [42] M. KLOTZ, M. H.: Lasersensorik in Partikelzählern: Schlüssel zur Optimierung des Partikelmonitoring. In: *GIT* 49 (2005), Nr. 9, S. 774–777
- [43] *PAMAS: PAMAS HCB-LD brochure*. http://pamas.de/content/download/1013/10835/HCB-LD_e_screen.pdf
- [44] HEATH, Alex R. ; FAWELL, Phillip D. ; BAHRI, Parisa A. ; SWIFT, Jean D.:

Estimating average particle size by focused beam reflectance measurement (FBRM).
In: *Particle & Particle Systems Characterization* 19 (2002), Nr. 2, S. 84–95

- [45] *Arduino: Language reference*. <http://arduino.cc/en/Main/ArduinoBoardUno>
- [46] *Relaisplatine REL-PCB4 mit Relais 5 V/DC-Spule Conrad REL-PCB4 1 5 V/DC 1 Wechsler 50 W/110 VA*. http://www.produktinfo.conrad.com/datenblaetter/500000-524999/503328-an-01-ml-Relaisplatine_REL_PCB4_5VDC_de_en_fr_nl.pdf
- [47] *Klotz Laser-sensors LDS for particle measurement*. <http://fa-klotz.de/media/produkte/produkt-flyer-pdf/4549-2seiter-lasersensoren-en-klotz.pdf>
- [48] *Klotz USB Box, Evaluation unit for LDS sensors for connecting to a PC (USB interface)*. <http://fa-klotz.de/media/produkte/produkt-flyer-pdf/4331-2seiter-usbbox-en-klotz-monitor.pdf>
- [49] BESENHARD, M. O. ; HOHL, R. ; HODZIC, A. ; EDER, R. J. P. ; KHINAST, J. G.: Modeling a seeded continuous crystallizer for the production of active pharmaceutical ingredients. In: *Crystal Research and Technology* 49 (2014), Nr. 2-3, S. 92–108
- [50] *Matlab: Arduino Support from MATLAB*. <http://www.mathworks.de/hardware-support/arduino-matlab.html>
- [51] *Arduino: Language reference*. <http://arduino.cc/en/Reference/HomePage>
- [52] *Hygrosens DRTR-AL-10V-R1B6: data sheet*. http://www.produktinfo.conrad.com/datenblaetter/500000-524999/502073-da-01-en-DRUCKTRANSMITTER_10_V__0___1_6_BAR.pdf
- [53] MYERSON, Allan: *Handbook of industrial crystallization*. Butterworth-Heinemann, 2002

Appendix

Import for 16 Channel mode

```
1 % calculates distributive and cummulative data for CSD measurements in
2 % 4096 Channel mode
3 %-----
4 function data_16 = call16(data)
5
6 % relative frequency distribution
7 for i=1:length(data)
8     data_16(i,1)=data(i);
9 end
```

Import for 4096 Channel mode

```
1 % calculates distributive and cummulative data for CSD measurements in
2 % 4096 Channel mode
3 % taken *.ops files contains relative frequency of each measured
4 % particle size; each size consists of a different number of channels
5 %
6 %-----
7 function data_4096 = cal4096(data)
8 %indices of particle size between 5-495µm in *.ops files
9 index = [294,1179,1761,1957,2154,2290,2366,2443,2519,2595,2661,...
10         2715,2770,2825,2879,2933,2988,3043,3097,3152,3198,3235,3273,...
11         3310,3348,3385,3423,3461,3498,3536,3569,3599,3629,3658,3688,...
12         3717,3747,3777,3807,3836,3863,3886,3909,3932,3956,3979,4002,...
13         4025,4048,4072];
14
15 index = index+1;
16
17 data_4096 = zeros(length(index),1);
18
19 %sum distributed values to size-classes
20 for(i = 1:length(index))           %loop size classes
21     index_cur = index(i);
22     if i ~= length(index)
23         index_next = index(i+1)-1;
24     else
25         index_next = 4096;         %last index value
```

```

26     end
27
28     for j =index_cur:index_next
29         %sum up distributed values
30         data_4096(i,1) = data_4096(i,1) + data(j);
31     end
32 end
33
34 %calculate cummulative values
35 data_4096(1,2) = sum(data_4096(:,1));
36 for k=1:length(data_4096)
37     if k == length(data_4096)
38         data_4096(k,2) = data_4096(k,1);
39     else
40         data_4096(k+1,2) = data_4096(k,2)-data_4096(k,1);
41     end
42 end

```

Data Import

```

1 % Import file list and gives as output cummulative histogram,
2 % distributive histogram and measured particle size
3 % usable for channel mode 16/4096; mode 4096 only for particle size
4 % from 5-495µm in 10µm steps
5 % -----
6 function [control_data_cum, control_data_dis, particle_size] = ...
7     data_import(files,num_measure)
8 %% Import data
9     num_even=1; %indices variable
10    control_data_dis = zeros(50,num_measure); %preallocate
11    variable
12
13    %odd files are measurement files, in case last file in
14    %dictionary is particle measurement
15    if mod(max(size(files)),2) ~= 0
16        for i=0:num_measure-1
17            data = importdata(files(end-(i*2)).name,',' );
18            data1 = data.data(:,2);
19
20            %Get particle size values and mode
21            char_text = char(data.textdata(5,1));

```

```

22     sep_text = regexp(char_text, ' ', 'split');
23     particle_size = cellfun(@str2double, sep_text(1, 2:end));
24
25     if length(particle_size) == 16
26         mode = '16';
27     else
28         mode = '4096';
29     end
30
31     switch mode
32         case '16'
33             %Calculation for 16Channel
34             %dist.(1) /cum.(2) histogram of particle size
35             data_16 = call16(data1);
36             control_data_dis(:, i+1) = data_4096(:, 1);
37             control_data_cum(:, i+1) = data_16(:, 2);
38
39             case '4096'
40             %4096Channel measurement with 5µm-495µm
41             data_4096 = cal4096(data1);
42             control_data_dis(:, i+1) = data_4096(:, 1);
43             control_data_cum(:, i+1) = data_4096(:, 2);
44         end
45     end
46     else
47         for i=1:2:(num_measure*2)-1
48             data = importdata(files(end-i).name, ';');
49             data1 = data.data(:, 2);
50
51             %Get particle size values and mode
52             char_text = char(data.textdata(5, 1));
53             sep_text = regexp(char_text, ' ', 'split');
54             particle_size = cellfun(@str2double, sep_text(1, 2:end));
55
56             if length(particle_size) == 16
57                 mode = '16';
58             else
59                 mode = '4096';
60             end
61
62             switch mode
63                 case '16'

```

```

64         %Calculation for 16Channel
65         data_16 = call16(data1);
66         control_data_dis(:,num_even) = data_16(:,1);
67         control_data_cum(:,num_even) = data_16(:,2);
68         num_even = num_even+1;
69
70         case '4096'
71             %4096Channel measurement with 5µm-495µm
72             data_4096 = cal4096(data1);
73             control_data_dis(:,num_even) = data_4096(:,1);
74             control_data_cum(:,num_even) = data_4096(:,2);
75             num_even = num_even+1;
76         end
77     end
78 end

```

Data acquisition/evaluation and control system

```

1  %% CSD measurement and control pump rate
2  clc
3  clear all
4  close all
5  %% Input Settings
6  %desired particle size
7  ref_size = str2double(input('Define Referenz Size: \n','s'));
8  %maximal variance of final particle size to desired size
9  max_variance = str2double(input('Define Maximal variance: \n','s'));
10
11 %fines boundery see indices in particle_size variable
12 fines_bound_low = 4;
13 %4...35µm  43...425µm
14 fines_bound_up = 43;
15 %number of used particle for calculation
16 num_particle = fines_bound_up-fines_bound_low+1;
17
18 %define number of classes for chi test ~ 5*log(n) n... total particle
19 class = 20;
20 class_array = (1:class);
21 %number of used particle size for each class
22 delta_class = num_particle/class;
23
24 %define number of measurements to be used for calculation, starting

```

```

25 %with last measurement
26 num_measure = 3;
27 %max.deviation of measured mean-particle size for consistency test
28 mean_tresh = 5;
29 Kp = 0;
30
31 % Constant variable
32 tube_length = 15; %tube length in m
33 tube_vol = ((0.2/2)^2)*pi*tube_length*100; %Volume of total tube in
    cm
34 pump_feed = 20; %ml/min
35
36 %% Initiate with first desired particle size
37 cal_cur=[141.8 129.35 118.075 106.8 101.7 96.6 92.655 89.11];
38
39 Controller start
40 tmp = abs(cal_cur-ref_size);
41 [idx idx] = min(tmp); %index of closest value
42
43 if idx+2 < 10
44     cur_pump_rate = idx+2;
45     cur_pump_rate_set = ['1f' '0' num2str(cur_pump_rate*100) '-2'];
46     disp(cur_pump_rate_set)
47     fprintf(pump,cur_pump_rate_set);
48 else
49     cur_pump_rate = idx+2;
50     cur_pump_rate_set = ['1f' num2str(cur_pump_rate*100) '-2'];
51     disp(cur_pump_rate)
52     fprintf(pump,cur_pump_rate_set);
53 end
54
55 %time trough process in s
56 time_pro = tube_vol/((pump_feed+cur_pump_rate)/60);
57
58 sampling_time = 10; %update frequency in s
59 wash_duration = 84+time_pro;
60 % status variable
61 %status of controller 0... not in use 1... in use
62 controller_status = 0;
63 %internal clock for rest of time after starting with process washing
64 rest_time = 0;
65

```

```

66 %% Setup Pump
67 pump = serial('COM3','Terminator','CR');
68 fopen(pump);
69 fprintf(pump,'1H');
70
71 %Acoustic alarm for controller
72 tone_a=sin(2*pi*440*(0:0.000125:0.25));
73 tone_d=sin(2*pi*587.33*(0:0.000125:0.25));
74
75 index_error = 1;
76 %recoding deviation of desired size and measured size
77 filename_error = '14-05-27_deltasize';
78
79 %% Continious measurement
80 H = uicontrol('Style', 'PushButton', 'String', 'Stop', 'Callback', ...
81             'delete(gcf)');
82
83 while (ishandle(H))
84
85 %load status variable of process; status 1/2/3 for process in wash-mode
86     ,
87 % 0 for feed in process
88     load('C:\klotz\Eigene Dateien\MATLAB\status.mat')
89
90     if status_val_pro == 0 || status_val_pro == 1 || ...
91         status_val_pro == 2 || status_val_pro == 3
92
93         folder_name = 'Y:\Measurements\Data\*.ops';
94         files = dir(folder_name);
95
96         %loop until necessary number of measurements are reached
97         while length(files) < num_measure*2
98             files = dir(folder_name);
99             pause(sampling_time)
100             disp('Not enough files')
101         end
102
103 %% Import data
104     % order: first column = last measurement;
105     [control_data_cum, control_data_dis, particle_size] = ...
106         data_import(files, num_measure);

```

```

107 %% Calculation Q0/Q1/Q2/Q3
108 %preallocating variables
109
110 % Distribution data
111 q0_data = zeros(fines_bound_up+1-fines_bound_low,num_measure);
112 q0_mean = zeros(num_measure,1);
113 % Class data for chi-square test
114 q0_data_class = zeros(class,num_measure);
115 q0_mean_class = zeros(1,num_measure);
116 q0_var_class = zeros(1,num_measure);
117 % Parameter calculation
118 q0_sigma = zeros(1,num_measure);
119 q0_mu = zeros(1,num_measure);
120
121 lognorm_q0 = zeros(class,num_measure);
122
123 chi_values_mod = zeros(4,num_measure);
124
125 dif_mean = zeros(num_measure,1);
126
127 for i=1:num_measure
128
129     %Q0 + mean particle size calculation
130     q0_data(:,i) = control_data_dis(fines_bound_low:fines_bound_up,i)
131     ...
132     ./sum(control_data_dis(fines_bound_low:fines_bound_up,i));
133     q0_mean(i) = sum(q0_data(:,i).*particle_size(fines_bound_low:...
134     fines_bound_up)');
135
136     %Q0 classes histogram
137     ind_class = 1;
138     for k=1:delta_class:delta_class*class
139         q0_data_class(ind_class,i) = sum(q0_data(k:k+delta_class-1,i));
140         ind_class = ind_class+1;
141     end
142
143     %parameter calculate for model distribution function for chi-test
144     % assumption that measurements are log-normal distributed
145
146     %mean value of log-normal distributed function
147     q0_mean_class(i) = sum(q0_data_class(:,i).*(1:class)');
148     %variance of log-normal distributed function
149     q0_var_class(i) = (1/(class-1))*sum((class_array-...

```

```

148     q0_mean_class(i)).^2);
149     %mu and sigma of normal-distributed function
150     q0_sigma(i) = sqrt(log(1+(q0_var_class(i)/...
151         (q0_mean_class(i)^2)))));
152     q0_mu(i) = log(q0_mean_class(i))-((q0_sigma(i)^2)/2);
153     %generate log-normal distrubtion as expected values for chi-test
154     % not normed
155     lognorm_q0(:,i)=lognpdf(class_array,q0_mu(i),q0_sigma(i));
156     %normalize expected values to 1
157     lognorm_q0(:,i)=lognorm_q0(:,i)/sum(lognorm_q0(:,i));
158
159     %Chi-square-test regard to expected shape of distribution using
160     % a lognorm-distribution model --> outlier detector
161     chi_values_mod(1,i) = sum(((q0_data_class(:,i)-...
162         lognorm_q0(:,i)).^2)./lognorm_q0(:,i));
163 end
164
165 %% Test cases
166 %test variable; 1... mean, 2... chi-shape, 3... chi-value2value
167 test_status = zeros(3,1);
168
169 %calculate difference between the mean value of one CSD
170 % with the mean value of the last three CSD measurement
171 for i=1:num_measure
172     dif_mean(i) = q0_mean(i)-mean(q0_mean);
173 end
174
175 %test cases
176 %case: mean
177 if abs(dif_mean) < mean_tresh
178     test_status(1) = 1;
179 end
180
181 %case: chi-shape measurement to model
182 if chi_values_mod(1,:) < 1
183     test_status(2) = 1;
184 end
185
186 %case: number of particles < 30k
187 if sum(q0_data./3) < 30000
188     test_status(3) = 1;
189 end

```

```

190
191 %% Controller
192 %get in Controller when test cases are passed
193 if sum(test_status) == 3
194 %controller start only one time per cycle necessary to avoid update
195 % of pumprate within a cylce; status 0 ... controller off
196 if controller_status == 0
197 %delta-size
198 error = mean(q0_mean)-ref_size;
199 error_values(index_error) = error;
200 save(filename_error,'error_values')
201 disp(['Current Pump-rate = ',num2str(cur_pump_rate)])
202 disp(['Current particle size = ',num2str(mean(q0_mean))])
203 disp(['Delta size = ',num2str(error)])
204 index_error = index_error+1;
205 %error not within final particle size range
206 if abs(error) > max_variance
207     if error > 0
208         %reference size smaller then current size -> Using Kp
209         cur_pump_rate = controller(cur_pump_rate,error)*(1-Kp);
210         disp(['New Pump-rate = ',num2str(cur_pump_rate)])
211     else
212         if controller(cur_pump_rate,error) >= 1
213             %reference size bigger then current size -> Using Kp
214             cur_pump_rate = controller(cur_pump_rate,error)*(1+Kp);
215             disp(['New Pump-rate = ',num2str(cur_pump_rate)])
216         else
217             cur_pump_rate = 1;
218             disp(['New Pump-rate = ',num2str(cur_pump_rate)])
219         end
220     end
221
222     if cur_pump_rate < 10 && cur_pump_rate >= 1
223         cur_pump_rate_set = num2str(round(cur_pump_rate*100));
224         cur_pump_rate_set = ['1f' '0' cur_pump_rate_set '-2'];
225         %flow-rate, 1fxxxx-2 e.g. 1f1200-2 means 12ml/min
226         fprintf(pump,cur_pump_rate_set);
227         disp(cur_pump_rate_set)
228         sound([tone_a,tone_d,tone_a,tone_d])
229     elseif cur_pump_rate < 1
230         cur_pump_rate_set = num2str(round(cur_pump_rate*100));
231         cur_pump_rate_set = ['1f' '00' cur_pump_rate_set '-2'];

```

```

232         fprintf(pump, cur_pump_rate_set);
233         disp(cur_pump_rate_set)
234         sound([tone_a,tone_d,tone_a,tone_d])
235     else
236         cur_pump_rate_set = num2str(round(cur_pump_rate*100));
237         cur_pump_rate_set = ['1f' cur_pump_rate '-2'];
238         fprintf(pump, cur_pump_rate_set);
239         disp(cur_pump_rate_set)
240         sound([tone_a,tone_d,tone_a,tone_d])
241     end
242     controller_status = 1;
243 else
244     disp('HURREY')
245     if strcmp(input...
246         ('New Size ? Type yes for continue \n', 's'), 'yes') == 1
247         ref_size = str2double(input...
248             ('Define new Referenz Size: \n', 's'));
249         max_variance = str2double(input(...
250             'Define new maximal variance to desired size \n', 's'));
251     else
252         fclose(pump);
253         save(filename_error, 'error_values')
254         return
255     end
256 end
257 end
258 end
259 %% Plot Qx-Distribution
260 %Plot Q0 CSD measurements, normalized histogram Q0
261 figure(1)
262 subplot(2,1,1)
263 plot(particle_size(fines_bound_low:fines_bound_up), ...
264     q0_data(:, :). *100)
265 xlabel('Particle Size [ $\mu$ m]')
266 ylabel('Q0 [%]')
267 xlim([particle_size(fines_bound_low) ...
268     particle_size(fines_bound_up)])
269 subplot(2,1,2)
270 t = linspace(56, 56*num_measure, num_measure); %./60;
271 plot(t, q0_mean(end:-1:1), 'ro')
272 j=1;
273 for i=56:56:56*num_measure

```

```

274     text(i, q0_mean(end+1-j), num2str(round(control_data_cum...
275         (1, end+1-j)/1000)))
276     j=j+1;
277 end
278 xlabel('Time [s]')
279 ylabel('Average diameter [ $\mu$ m]')
280 print(figure(1), '-djpeg', 'Q0.jpg');
281
282 %%
283 if controller_status == 1
284     disp('Controller worked - waiting to next cycle')
285     pause(sampling_time)
286 else
287     disp('Controller not worked - test cases not complete')
288     disp(test_status)
289     pause(sampling_time)
290 end
291
292 if status_val_pro == 1 || status_val_pro == 2 || ...
293     status_val_pro == 3
294     disp('PROCESS IN WASH-MODE')
295     rest_time = rest_time + sampling_time;
296     %time_sample = rest time of existing particles in reactor
297     if rest_time > time_pro
298         %controller ready for next cycle
299         controller_status = 0;
300         rest_time = 0;
301         %pause of etoh
302         pause(wash_duration)
303     end
304 elseif rest_time ~= 0
305     rest_time = rest_time + sampling_time;
306     if rest_time > time_pro
307         controller_status = 0;
308         rest_time = 0;
309         pause(wash_duration)
310     end
311 end
312
313 else
314     disp('Process not starting')
315     %update until process starts

```

```

316     pause (sampling_time)
317 end
318 end

```

Valve control script

```

1  Script for the control of the valve systems and pressure measurement
2  % within the tubular crysallizer
3  % Valve and pressure sensor control 1.0
4  clc
5  clear all
6
7  %% SETUP DEVICES
8  %Setup Arduino Board
9  ard = arduino('COM4');
10 pinMode(ard,9,'OUTPUT')           %sample valve at detector unit
11 pinMode(ard,10,'OUTPUT')         %wash valve at detector unit
12 pinMode(ard,5,'OUTPUT')         %
13 pinMode(ard,6,'OUTPUT')
14
15 %% SETUP used parameter
16 %set Number of measurements
17 num_cycl = str2double(input('Number of measurements \n','s'));
18 %set time duration of opened sample valve
19 mea_time = str2double(input('Measuring Time \n','s'));
20 %set time duration of opened wash solution valve
21 wash_time = str2double(input('Washing Time \n','s'));
22
23 i=1;
24 %status variable of valve system at detector unit;
25 % 0 closed wash/opened sample
26 status_val_sen = 0;
27 %status variable of crystallizer; cleaning stops with value 3,
28 % value changes to 1/2/3 when timepoint is reached
29 status_val_pro = 0;
30 %treshhold value for pressure sensor
31 pres_treshhold = 1500;
32 %timepoint for rinsing the tubular crystallizer with wash solution
33 wash_process = 420;
34 %intern clock
35 expired_time = 0;
36

```

```

37 %Alarm
38 tone_a=sin(2*pi*440*(0:0.000125:0.25));
39 tone_d=sin(2*pi*587.33*(0:0.000125:0.25));
40
41 %Status variable of process
42 savefile = 'status.mat';
43 %Recording pressure data
44 filename = '14-06-03_pres_bar_pro8_eqweqe4';
45
46 while i ~= num_cycl*2+2      %measurements begin with 3rd valve switch
47     if i == 1
48         %Initial of sample probe to detector (slurry is not already in track)
49
50         digitalWrite(ard,10,1)    %close wash valve at detector unit
51         digitalWrite(ard,9,1)    %open sample valve at detector unit
52
53         %read out pressure data
54         pres = analogRead(ard,0);
55         %values in mbar, value 1.568 resolution per unit
56         pres_bar(i) = 1.568*pres;
57         disp(['Current pressure = ',num2str(1.568*pres)])
58         save(filename,'pres_bar')
59
60         %Acoustic alarm at too high presse within the crysallizer
61         if pres_bar > pres_treshhold
62             msgbox('PROCESS BLOCKING')
63             sound([tone_a,tone_d,tone_a,tone_d])
64         end
65
66         status_val_sen = 1;
67         i = i+1;
68         time = mea_time+6;
69         save(savefile, 'status_val_pro')    %update of status variable
70         pause(time)                        %+20sec Wegstrecke
71         expired_time = expired_time+time;  %intern clock
72     else
73         if status_val_sen == 0
74             digitalWrite(ard,10,1)    %close wash valve at detector unit
75             digitalWrite(ard,9,1)    %open sample valve at detector unit
76
77             pres = analogRead(ard,0);
78             pres_bar(i) = 1.568*pres;

```

```

79     disp(['Current pressure = ', num2str(1.568*pres)])
80     save(filename, 'pres_bar')
81
82     if pres_bar > pres_treshhold
83         msgbox('PROCESS BLOCKING')
84         sound([tone_a,tone_d,tone_a,tone_d])
85     end
86
87     status_val_sen = 1;
88     i = i+1;
89     time = mea_time+3;
90     save(savefile, 'status_val_pro')
91     pause(time)
92     expired_time = expired_time+time;
93
94     if status_val_pro == 3
95         digitalWrite(ard,5,0)
96         digitalWrite(ard,6,0)
97         status_val_pro=0;
98         expired_time = 0;
99         disp('Process purging stopped')
100        save(savefile, 'status_val_pro')
101    end
102
103    if wash_process < expired_time
104        %close valve of feed solution
105        digitalWrite(ard,5,1)
106        %open valve for cleaning crystallizer
107        digitalWrite(ard,6,1)
108        status_val_pro = status_val_pro+1;
109        disp('Process purging starting')
110        save(savefile, 'status_val_pro')
111    end
112    else
113        digitalWrite(ard,10,0)        %close Valve II
114        digitalWrite(ard,9,0)        %open Valve I
115
116        pres = analogRead(ard,0);
117        pres_bar(i) = 1.568*pres;
118        disp(['Current pressure = ', num2str(1.568*pres)])
119        save(filename, 'pres_bar')
120

```

```

121     if pres_bar > pres_treshhold
122         msgbox('PROCESS BLOCKING')
123         sound([tone_a,tone_d,tone_a,tone_d])
124     end
125
126     status_val_sen = 0;
127     i = i+1;
128     time = wash_time+3;
129     save(savefile, 'status_val_pro')
130     pause(time)
131     expired_time = expired_time+time;
132
133     if status_val_pro == 3
134         digitalWrite(ard,5,0)    %open valve for feed solution
135         digitalWrite(ard,6,0)    %close valve for cleaning crystallizer
136         status_val_pro=0;
137         expired_time = 0;
138         disp('Process purging stopped')
139         save(savefile, 'status_val_pro')
140     end
141
142     if wash_process < expired_time
143         digitalWrite(ard,5,1)    %close valve of feed solution
144         digitalWrite(ard,6,1)    %open valve for cleaning crystallizer
145         status_val_pro = status_val_pro+1;
146         disp('Process purging starting')
147         save(savefile, 'status_val_pro')
148     end
149 end
150 end
151 end

```